A COMPARISON OF WATERFLOOD MANAGEMENT USING ARRIVAL TIME OPTIMIZATION AND NPV OPTIMIZATION

A Thesis

by

QING TAO

Submitted to the Office of Graduate Studies of
Texas A&M University
in partial fulfillment of the requirements for the degree of

MASTER OF SCIENCE

December 2009

Major Subject: Petroleum Engineering

A COMPARISON OF WATERFLOOD MANAGEMENT USING ARRIVAL TIME OPTIMIZATION AND NPV OPTIMIZATION

A Thesis

by

QING TAO

Submitted to the Office of Graduate Studies of
Texas A&M University
in partial fulfillment of the requirements for the degree of

MASTER OF SCIENCE

Approved by:

Chair of Committee,	Akhil Datta-Gupta
Committee Members,	Behnam Jafarpour
	Bani Mallick
Head of Department,	Stephen A. Holditch

December 2009

Major Subject: Petroleum Engineering

ABSTRACT

A Comparison of Waterflood Management Using Arrival Time Optimization and NPV Optimization. (December 2009)

Qing Tao, B.S., Tsinghua University

Chair of Advisory Committee: Dr. Akhil Datta-Gupta

Waterflooding is currently the most commonly used method to improve oil recovery after primary depletion. The reservoir heterogeneity such as permeability distribution could negatively affect the performance of waterflooding. The presence of high permeability streaks could lead to an early water breakthrough at the producers and thus reduce the sweep efficiency in the field. One approach to counteract the impact of heterogeneity and to improve waterflood sweep efficiency is through optimal rate allocation to the injectors and producers. Through optimal rate control, we can manage the propagation of the flood front, delay water breakthrough at the producers and also increase the sweep and hence, the recovery efficiency. The arrival time optimization method uses a streamline-based method to calculate water arrival time sensitivities with respect to production and injection rates. It can also optimize sweep efficiency on multiple realizations to account for geological uncertainty. To extend the scope of this optimization method for more general conditions, this work utilized a finite difference simulator and streamline tracing software to conduct the optimization.

Apart from sweep efficiency, another most widely used optimization method is to maximize the net present value (NPV) within a given time period. Previous efforts on optimization of waterflooding used optimal control theorem to allocate injection/production rates for fixed well configurations. The streamline-based approach gives the optimization result in a much more computationally efficient manner.

In the present study, we compare the arrival time optimization and NPV optimization results to show their strengths and limitations. The NPV optimization uses a perturbation method to calculate the gradients. The comparison is conducted on a 4-spot synthetic case. Then we introduce the accelerated arrival time optimization which has an acceleration term in the objective function to speed up the oil production in the field. The proposed new approach has the advantage of considering both the sweep efficiency and net present value in the field.

DEDICATION

To my beloved wife and parents for their selfless encouragement and support.

ACKNOWLEDGEMENTS

I would like to express my gratitude to my graduate advisor, Dr. Akhil Datta-Gupta, for his insightful guidance in my research and educational development. I would like to thank my committee members, Dr. Behnam Jafarpour and Dr. Bani Mallick, for their valuable comments and discussions. I would also like to thank my senior student, Ahmed Alhuthali, and other labmates for their constructive suggestions and discussions in the completion of my research.

TABLE OF CONTENTS

Page

LIST OF FIGURES

FIGURE Page

LIST OF TABLES

1. INTRODUCTION

1.1 Literature Review

The high worldwide oil demand requires that we need to efficiently produce existing oil fields. A variety of secondary oil recovery methods has been developed to improve oil recovery after primary depletion (Lake et al. 1992; Craig 1971). The most widely used is waterflooding because it is relatively easy and inexpensive to implement. The reservoir heterogeneity such as permeability field could negatively affect the performance of waterflooding. The presence of high permeability streaks could lead to an early water breakthrough at the producers and thus reduce the sweep efficiency in the field. (Sudaryanto and Yortsos 2001; Brouwer et al. 2001; Brouwer and Jasen 2004; Alhuthali et al. 2007). Various methods have been suggested to mitigate this problem. Among these is smart well completions where the production or the injection section is divided into several intervals (Arenas and Dolle 2003; Glandt 2003; Hussain et al. 2005). The flow rate at each interval can be independently controlled by inflow control valves (ICVs); hence, making it possible to control flow rates across the high permeability streaks.

The appealing features of the smart well technology have inspired several researchers to develop efficient algorithms to optimize production along the intervals of smart wells, and thereby improve sweep efficiency. Two main types of optimization algorithms were developed, namely the gradient-based algorithms and the stochastic algorithms (Brouwer and Jasen 2004; Sarma et al. 2005; Tavakkolian et al. 2004;

This thesis follows the style of *SPE Journal*.

Emerick et al. 2007). Both algorithms use reservoir simulators to evaluate the objective function. The gradient-based algorithms require an efficient estimation of the gradient of the objective function with respect to the control variables. In contrast, the stochastic algorithms such as genetic algorithms do not require an estimation of the gradient, but they require multiple forward simulation runs to find the global minimum.

The approach developed by Alhuthali (2007, 2008 and 2009) has proves on various synthetic and field cases to counteract the impact of heterogeneity and to improve waterflood sweep efficiency. The underlying idea is to equalize the arrival time of the waterfront at the producers through optimal rate allocation. The arrival time optimization has favorable quasi-linear properties and the optimization proceeds smoothly even if the initial conditions are far from the solution (Cheng et al. 2005a). Furthermore, the sensitivity of the arrival time with respect to injection and production rates can be calculated analytically using a single flow simulation. This makes the approach computationally efficient and suitable for large-scale field applications. The arrival time optimization ensures appropriate rate allocation and flood front management by delaying the water breakthrough at the producing wells. This approach is also generalized to account for geologic uncertainty since reservoir parameters such as permeability are known in a stochastic sense. The optimization problem is a constrained non-linear optimization, which is solved using sequential quadratic programming (SQP).

1.2 Objective of the Study

The main objective of this research is to compare the results between arrival time optimization and NPV optimization.

1.2.1 Introduction of Arrival Time Optimization and NPV Optimization

- The first step is to introduce the objective functions for both arrival time optimization and NPV optimization. Arrival time optimization maximizes the sweep efficiency in the field, while the NPV optimization gives the optimal result in an economic sense. The principle concept behind arrival time optimization is to equalize the arrival at all producers within a sub-group of wells. The objective function is formulated as the square of l_2 norm of the residuals between a desired arrival time and a calculated arrival time.
- The calculation of the gradients and Hessian of both optimization methods will be introduced. In arrival time optimization, the gradients and Hessian are computed analytically using an analytical form for the sensitivity of the arrival time with respect to the control variables (i.e. wells rates). The analytical computation of the gradient and Hessian will require only one simulation run. In NPV optimization, we use the perturbation method to calculate the gradients and Hessian numerically, using multiple simulation runs.
- The formulation of the accelerated arrival time optimization will also be introduced. In addition to the misfit of arrival time term, the new objective function will also have an acceleration term, which is the summation of arrival times in a sub-group. This can ensure that the arrival time optimization algorithm

not only improves sweep efficiency, but also accelerates oil production, which will lead to a high net present value comparable to the NPV optimization.

1.2.2 Arrival Time Optimization Case Study

- To address the effectiveness of arrival time optimization technique, we conduct this optimization algorithm on a 5-spot synthetic case as well as a field case. The arrival time optimization will improve the sweep efficiency in the field.
- Instead of using a streamline simulator to calculate the arrival times, we use a finite difference simulator for the simulation run. After the pressure field is updated, we trace streamlines using a post processor to get the arrival time information for the optimization algorithm. This is a more generalized technique and can be extended to more complicated applications such as compositional flow in future study.
- The optimization will be performed on multiple realizations to account for geological uncertainty. The gradients and the Hessian of the objective function will be computed analytically using only one simulation run per realization, which makes the approach efficient and suitable for large field cases.

1.2.3 Comparison of Arrival Time Optimization and NPV Optimization

- Both optimization schemes will be conducted on a 4-spot synthetic case. The comparisons will include contour maps of the objective functions, oil production profiles, net present values and so on. The advantages and limitations of both optimization techniques will be discussed.

- Accelerated arrival time optimization will also be conducted on this synthetic model. It can overcome the drawback of the previous arrival time optimization in the way that it can accelerate the production in the field. The net present value it generated is comparable to that of the NPV optimization, which proves its capability of optimizing both the sweep efficiency and net present value.

2. MATHEMATICAL FORMULATION AND APPROACH

In this section, we discuss the underlying mathematical formulations of the two optimization schemes.

2.1 Arrival Time Optimization

The formulation of the rate optimization is based on waterfront arrival times and the streamline time of flight. The sensitivities of arrival time to well rates are calculated analytically for the optimization process. Field and individual well constraints can be posted in the optimization process.

The main objective of arrival time optimization is to maximize sweep efficiency in the field through rate allocation. This can be achieved by minimizing the misfit between the desired arrival time and the calculated arrival time for a specific group of producers. For a single realization, we can formulate the objective function as the square of the L_2 norm of the residuals,

$$\left\|\mathbf{e}(\mathbf{q})\right\|_2^2 = \sum_{m=1}^{N_{group}} \sum_{i=1}^{N_{prod,m}} \left(t_{d,m} - t_{i,m}(\mathbf{q})\right)^2 \quad \text{.....(2.1a)}$$

where the arrival time residual at an individual well is given by

$$e_{i,m} = t_{d,m} - t_{i,m}(\mathbf{q}) \quad \text{..... (2.1b)}$$

The residuals are represented by the vector e in Eq. 2.1. The variable $t_{d,m}$ represents the desired arrival time for the group m. The calculated arrival time at well i, which belongs to group m, is denoted by $t_{i,m}$. The vector q contains the control variables and has a dimension of n, the number of well rates to be optimized.

We define the arrival time to a producer as the time required for the waterfront to reach its current position from the injector (Datta-Gupta 2007). For calculation purposes, we compute the arrival time to a producer as the average of the arrival times associated with a set of fast streamlines as defined by the user. In our application, we take the top 20% of the streamlines.

$$t_{i,m}^{k} = \left(\frac{1}{N_{fsl,i}} \sum_{l=1}^{N_{fsl,i}} \tau_{l,i} \Big/ \left[\frac{df_w}{dS_w} \right]_{S_w = S_{wf,l}} \right)^{k} \quad \text{..... (2.2)}$$

The desired arrival time for a group of producers is computed as the average of calculated arrival time at the producers within this group.

$$t_{d,m}^{k} = \frac{\sum_{i}^{N_{prod,m}} t_{i,m}(\mathbf{q}^{k})}{N_{prod,m}} \quad \text{..... (2.3)}$$

To address geologic uncertainty, the expected value for multiple realizations is given by:

$$\mathrm{E}\left[\mathbf{e}^{T}\mathbf{e}\right] = \frac{1}{Nr} \sum_{i=1}^{Nr} \mathbf{e}_i^{T}\mathbf{e}_i \quad \text{..... (2.4)}$$

The variable Nr in Eq. 2.4 refers to the number of realizations used in the optimization. Our goal is to minimize Eq. 2.4 by changing q, the injection or production rates, subject to multiple equality and inequality constraints which are mainly imposed by the operational restrictions and facility limitations.

$$\min_{\mathbf{q}} f(\mathbf{q}) \quad \text{..... (2.5)}$$

subject to

$$\mathbf{h}(\mathbf{q}) = 0$$
$$\mathbf{g}(\mathbf{q}) \le 0$$

where $h : \Re^n \to \Re^z$ and $g : \Re^n \to \Re^y$

To minimize the objective function, we use the sequential quadratic programming (SQP) algorithm which is one of the widely used algorithms for non-linear constrained optimization. The main concept behind it is to formulate the problem into a series of quadratic programming (QP) sub-problems which can be solved at major iteration k. The QP sub-problem is mainly a quadratic approximation of the Lagrangian of Eq. 2.5 which is given in the following form:

$$L(\mathbf{q}, \boldsymbol{\lambda}_L, \boldsymbol{\lambda}_K) = f(\mathbf{q}) + \boldsymbol{\lambda}_L^T \mathbf{h}(\mathbf{q}) + \boldsymbol{\lambda}_K^T \mathbf{g}(\mathbf{q}) \quad \text{..... (2.6)}$$

The vectors λ_L and λ_K refer to the Lagrange multipliers corresponding to the equality constraints. For our application, we assume that the constraints are linear and they have the following forms:

$$\mathbf{h(q)} = \mathbf{Aq} + \mathbf{b}$$
$$\mathbf{g(q)} = \mathbf{Cq} + \mathbf{d} \quad \text{..... (2.7)}$$

After linearization of the constraints using the first order Newton approximation, the QP sub-problem can be written as:

$$\min_{\mathbf{\delta q}} \left\|\mathbf{e}(\mathbf{q}^k) - \mathbf{S}(\mathbf{q}^k)\delta\mathbf{q}\right\|_2^2 + \left\|\beta\mathbf{\delta q}\right\|_2^2 \quad \text{..... (2.8)}$$

subject to

$$\mathbf{A}\delta\mathbf{q} + \mathbf{h}(\mathbf{q}^k) = 0$$
$$\mathbf{C}\delta\mathbf{q} + \mathbf{g}(\mathbf{q}^k) \le 0$$

In Eq. 2.8, $\delta\mathbf{q}$ represents a perturbation in rate and $\mathbf{S(q)}$ is the sensitivity matrix. A single entry of the sensitivity matrix S_{ij} quantifies the changes in arrival time at producer *i* because of small changes in the rate of well *j*. It is given by

$$S_{ij} = \frac{\partial t_{i,m}(\mathbf{q}^k)}{\partial q_j} \quad \text{..... (2.9)}$$

The Hessian of Eq. 2.8 is given by

$$\mathbf{H}^k = \mathbf{S}^T(\mathbf{q}^k)\mathbf{S}(\mathbf{q}^k) + \beta^2\mathbf{I} \quad \text{..... (2.10)}$$

The coefficients of the sensitivity matrix S_{ij} are computed analytically. The derivation of the analytical sensitivities is given in Appendix A. The final forms of the sensitivities with respect to production and injection rates are

$$S_{ij} = -\frac{t_{i,m}}{q_j} \quad \forall i = j$$
$$S_{ij} = 0 \quad \forall i \neq j \quad \text{.....(2.11a)}$$

where j is a producer.

$$S_{ij} = -\frac{\sum_{l=1}^{N_{fsl,i,j}} \tau_{l,i,j} \Big/ \left[\frac{df_w}{dS_w}\right]_{S_w=S_{wf,l}}}{q_j N_{fsl,i}} \quad if \quad N_{fsl,i,j} \neq 0 \qquad \text{(2.11b)}$$

$$S_{ij} = 0 \quad if \quad N_{fsl,i,j} = 0$$

where j is an injector.

In the above equation, we have substituted the water front arrival time in terms of the streamline time of flight and the saturation velocity. The variable $N_{fsl,i,j}$ is the number of the fast streamlines connecting a producer *i* to an injector *j*. This number represents only a portion of $N_{fsl,i}$, the total number of the fastest streamlines connected to the producer *i*. If the injector *j* is not connected to producer *i* through a fast streamline i.e. ($N_{fsl,i,j}$=0), then the arrival time at producer *i* is not sensitive to a perturbation in the rate of injector *j*.

The computation of the sensitivity matrix discussed here requires a single flow simulation using either a streamline or a finite-difference model. Use of finite-difference model will require the additional calculations associated with the streamlines and time of flight.

For multiple realizations case, the detailed derivation of the objective function formulation is in Appendix B.

The procedure for arrival time optimization is illustrated in Figure 2.1.

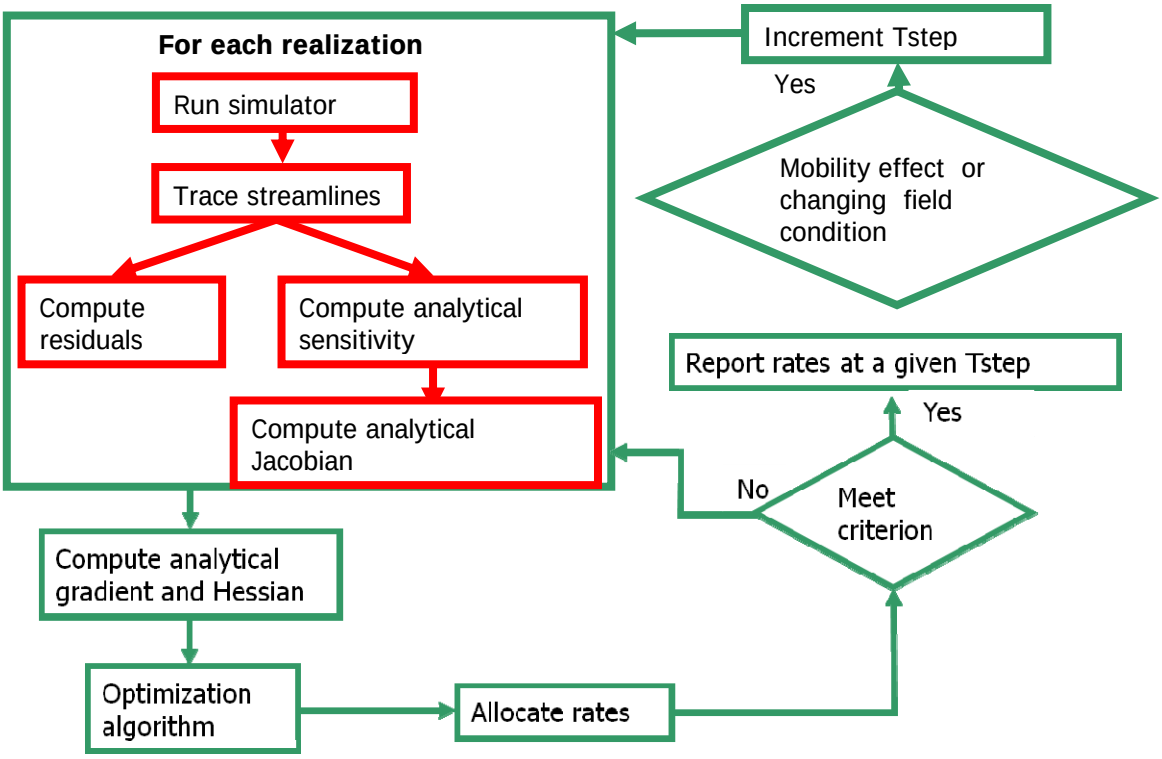

Figure 2.1 Work Flow of Arrival Time Optimization

The major steps of this approach are summarized as follows.

- Run the simulator and trace the streamlines for each realization.
- Compute the residuals, analytical sensitivities, and analytical Jacobian. The residuals quantify the misfit between the desired arrival time and the computed arrival time. This step involves the analytical computation of sensitivities for all realizations.
- Compute Analytical gradient and Hessian. This step is to use the analytical jacobian and the residuals to compute the gradient and the Hessian of the objective function analytically.

- Minimization and Optimal Rate Allocations. We used the Sequential quadratic programming (SQP) procedure to generate the required changes in rates to minimize the objective function.
- Mobility Effects and Changing Field Conditions. Once this criterion is met, we move to a new time interval, update streamlines and perform the optimization again to account for mobility effects and changing field conditions.

2.2 NPV Optimization

Another approach to optimize the waterflooding process is to maximize the objective function J which is defined as the net present value (NPV):

$$J = \sum_{k=0}^{K-1} \sum_{n=1}^{N_{pr}} \frac{r_o q_{o,n}(k) - r_{wp} q_{wp,n}(k) - r_{wi} q_{wi,n}(k)}{(1+b)^a} \Delta t(k) \quad \text{..... (2.12)}$$

Here, k is the time step counter, K is the total number of time steps in the simulation, n is the well segment counter, N_{pr} is the number of well segments in the producer, r_o is the oil price, r_w is the cost of water production, $q_{o,n}(k)$ and $q_{w,n}(k)$ are the oil and water rates at surface conditions at time step k in segment n, respectively, $\Delta t(k)$ is the time step size, 'b' is the discount rate, expressed as a fraction per year, and 'a' is the number of years passed since the start of production.

We use perturbation method to compute the sensitivities numerically in the control problem. The control variables are perturbed with a very small amount and the changes in the objective function value are recorded. The difference of the objective

function value over the perturbed amount will be the gradient of a certain control variable. The gradient of the objective function with respect to control parameter $u_i(k)$ is $\frac{dJ}{du_i(k)}$, where 'k' is the time step counter and 'i' is the index of control parameters. $du_i(k)$ could be a very small amount, for example 0.01, for the calculation of the gradients. The gradients in a matrix form can be expressed as:

$$\left[\frac{dJ}{du_1(1)} \quad \frac{dJ}{du_2(1)} \quad \cdots \quad \frac{dJ}{du_N(1)} \quad \cdots \quad \frac{dJ}{du_i(k)} \quad \cdots \quad \frac{dJ}{du_N(K)} \right] \text{..... (2.13)}$$

where K is the total number of time steps and N is the total number of control parameters.

The objective function and the gradients are fed into the optimization algorithm if we use a first order optimization algorithm, for example, steepest descent. If we use a second order optimization algorithm, the Hessein matrix will be necessary and it can also be calculated numerically.

Solution of the optimization problem consists of iterations until the optimal control vector $u_i(k)$ has been found for each time step.

The procedure for NPV optimization is illustrated in Figure 2.2.

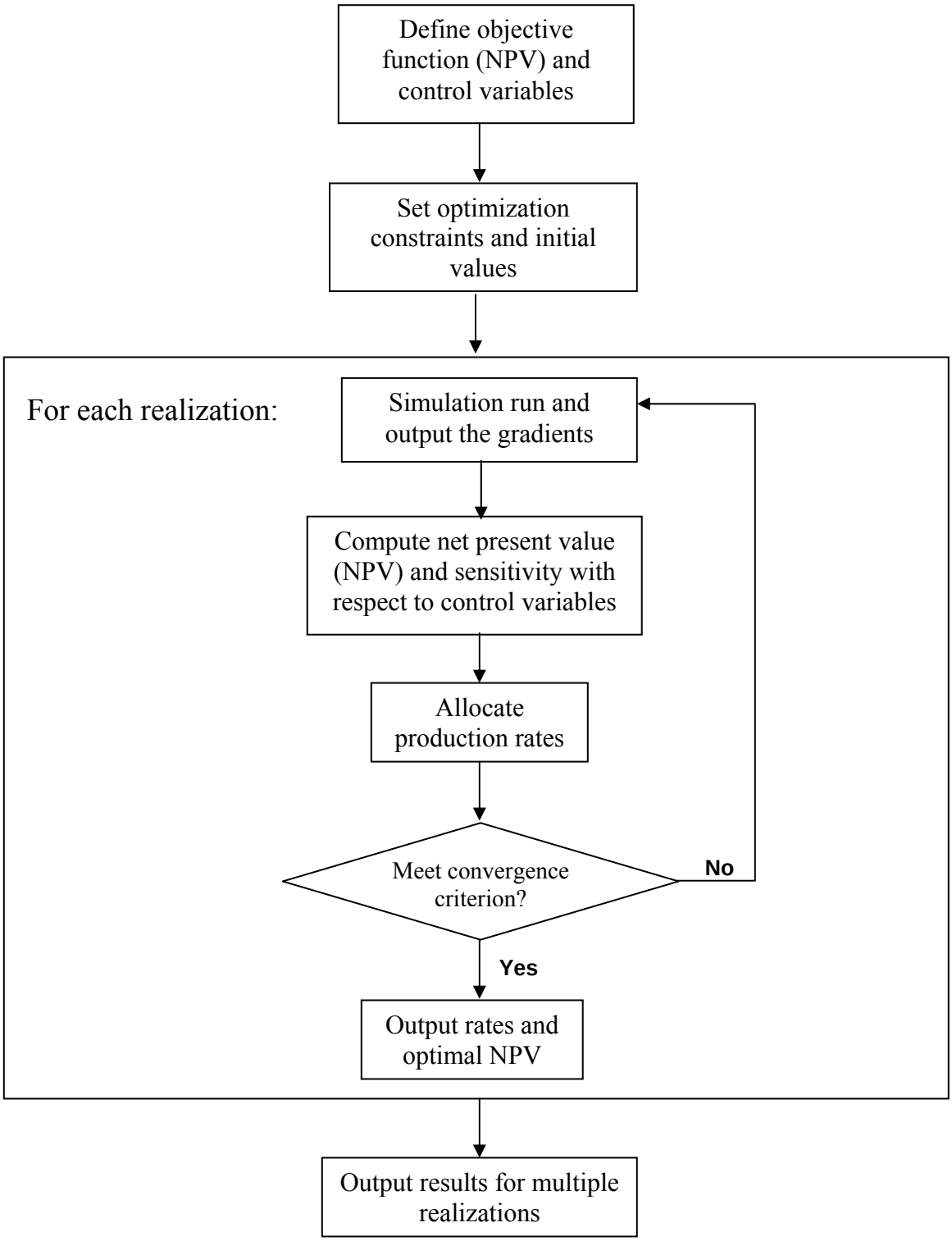

Figure 2.2 Work Flow of NPV Optimization

The major steps of the NPV optimization are summarized as follows.

- Set optimization objective function, control parameters and constraints. The control parameters and optimization constraints need to be carefully chosen according to the field characteristics. Those field and well production profiles should be realistic.
- Numerical simulation of the dynamic system behavior by solution of equations. This process is conducted by a reservoir simulator. In this study, ECLIPSE (2007) is used as the simulator.
- Calculate and output the NPV and its gradients with respect to control parameters. The NPV and its gradients are updated at each iteration. The gradients are calculated numerically using a perturbation method.
- Use an optimization algorithm, for example, steepest descent, to optimize the objective function by controlling the well parameters. The optimization algorithm will decide whether the result is accepted or not. If the result meets convergence criterion, the results will be output and the optimization goes to the next iteration.

2.3 Accelerated Arrival Time Optimization

The original arrival time optimization algorithm doesn't account for accelerated production strategy to maximize the net present value. We can add a norm constraint to the objective function to take care of the acceleration effect. The objective function can be written for a single realization as follows,

$$\left\|\mathbf{e}(\mathbf{q})\right\|_2^2 = \sum_{m=1}^{N_{group}} \sum_{i=1}^{N_{prod,m}} \left(t_{d,m} - t_{i,m}(\mathbf{q})\right)^2 + W \sum_{m=1}^{N_{group}} \sum_{i=1}^{N_{prod,m}} \left(t_{i,m}(\mathbf{q})\right)^2 \quad \text{..... (2.16)}$$

where the second term is the regularization term for production acceleration purpose. It represents the total arrival time and minimizing the second term in Eq. 2.16 will account for acceleration effects. Here, W is the weighting factor for the acceleration term. We will discuss in detail about the effect of the weighting factor in Section 4.

We are trying to solve the following optimization problem with the new objective function,

$$\min_{\mathbf{q}} \; f(\mathbf{q}) = \mathbf{e}^T\mathbf{e} + \mathbf{t}^T\mathbf{t} \,. \quad \text{..... (2.17)}$$

subject to

$$\mathbf{h}(\mathbf{q}) = 0$$
$$\mathbf{g}(\mathbf{q}) \le 0$$

where $h : \Re^n \to \Re^z$ and $g : \Re^n \to \Re^y$

The gradient of this objective has the following form,

$$\nabla_q \left[\mathbf{e}^T\mathbf{e}\right] = 2\left[\mathbf{J}^T\mathbf{e} + \mathbf{S}^T\mathbf{t}\right] \quad \text{..... (2.18)}$$

where J is the Jacobian of the misfit, and S is the sensitivity of the arrival time.

The Hessian can be written as,

$$\nabla_q^2 \left[\mathbf{e}^T\mathbf{e} + \mathbf{t}^T\mathbf{t}\right] = 2\left[\mathbf{J}^T\mathbf{J} + \mathbf{S}^T\mathbf{S}\right] \quad \text{..... (2.19)}$$

Those forms can be generalized to multiple realizations using the same procedures illustrated in Appendix B.

3. ARRIVAL TIME OPTIMIZATION CASE STUDY

The arrival time optimization approach is implemented in a finite-difference simulator. With finite-difference simulator, we need to perform the streamline tracing and time of flight computations using the total phase fluxes from the simulator (Cheng et al. 2005b). In addition, we assume that a static model is readily available and the injected fluid composition is fixed and it is not a control variable. The computation of the sensitivity matrix requires only one single flow simulation. Use of finite-difference model will require additional calculations associated with the streamlines and time of flight.

3.1 5-Spot Synthetic Case

A synthetic reservoir model was created to test our algorithms. The reservoir model consists of 50x50x1 gridblocks. The gridblocks are uniform 50x50x10 ft^3. The reservoir is composed of two phase, oil and water. The fluid composition and SCAL data are referred from the SPE9 data. The initial reservoir pressure is uniformly 3,600 psia and the initial water saturation is 0.2. The porosity of the field is assumed to be uniform at 0.2. The production scheme and permeability field is shown in Figure 3.1.

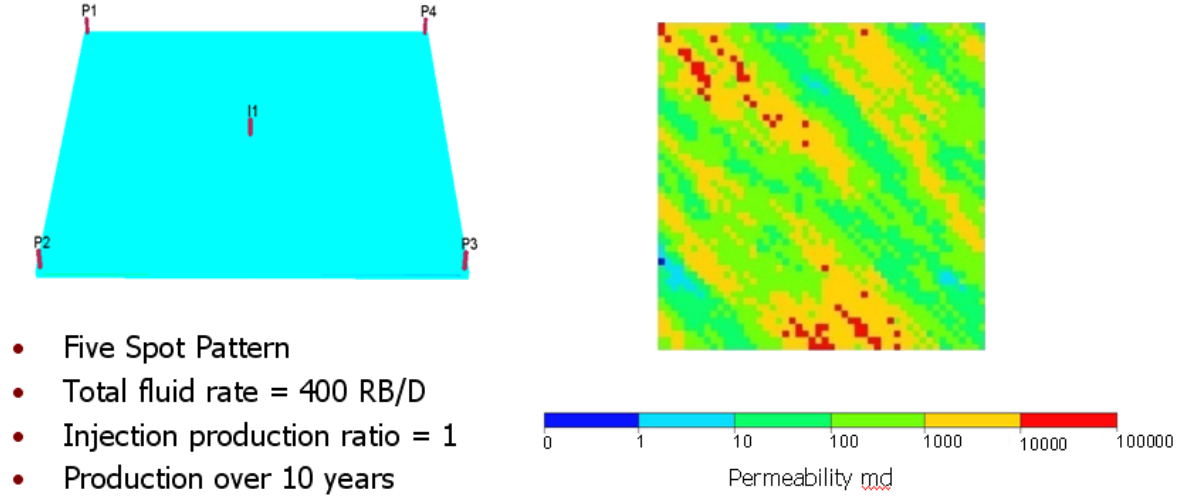

Figure 3.1 Well Configuration and Permeability Field of a 5-Spot Synthetic Case

We control the injection and production rates to be equal and conduct the optimization over 10 years period. To illustrate the effectiveness of this technique, we first plot the oil saturation maps for both the base case and the optimized case. The base case is a simulation run with equal rates for the producers. The field water breakthrough of the base case and optimized case are shown in Figures 3.2 and 3.3. From Figure 3.2, we can see that the water front distribution in the base case is not uniform due to the heterogeneity of the permeability field. At the end of the total production time period, the well in the bottom left still did not breakthrough which leads to large amounts of oil remaining in the field. However, if we use the arrival time optimization scheme to equalize the arrival time for every producer, the water breakthrough shows a much more uniform distribution, as shown in Figure 3.3. Therefore, the sweep efficiency in the field can be maximized. We can also check the results from Figures 3.4 to 3.6, which show

the comparison of cumulative oil production, water production and field water cut between the base case and the optimized case. The optimization scheme has successfully increased the oil production and decreased the water production in the field. At the same time, it delayed field water breakthrough from 1400 days to 2300 days.

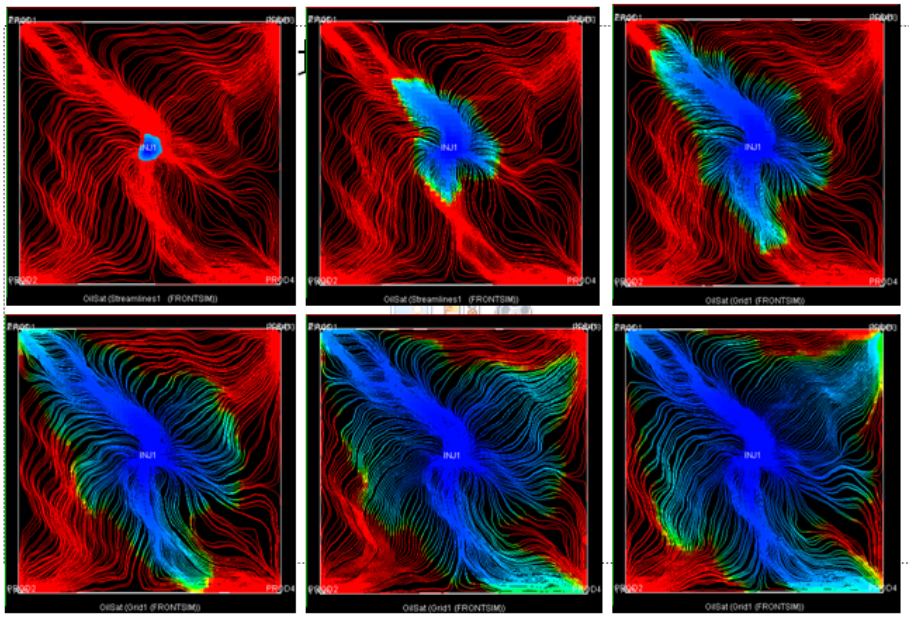

Figure 3.2 Oil Saturation Maps in the Base Case

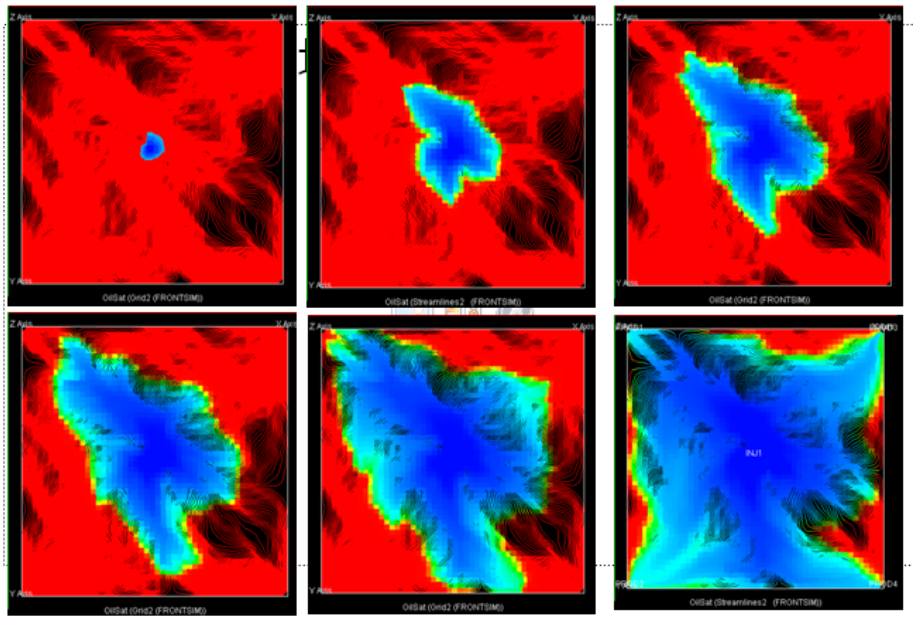

Figure 3.3 Oil Saturation Maps in the Optimized Case

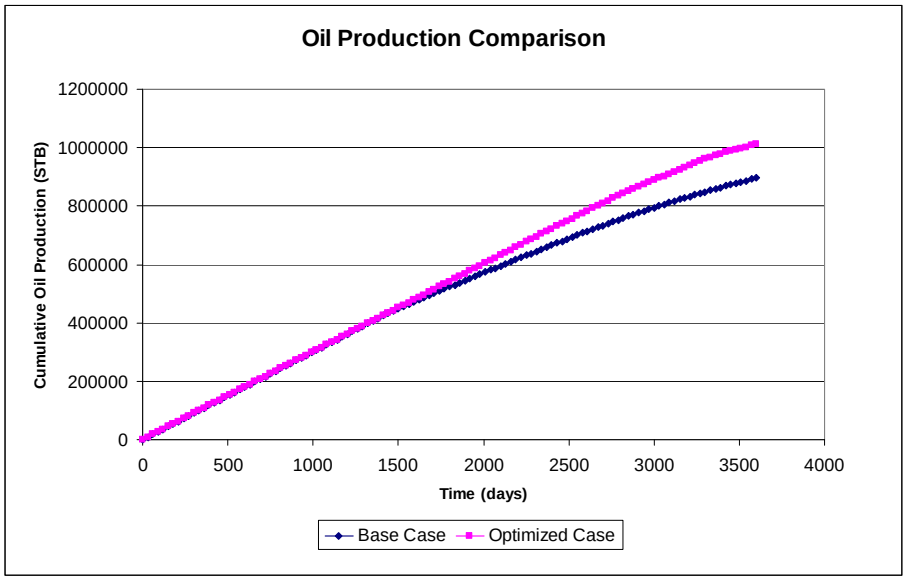

Figure 3.4 Comparison of Oil Production Profiles of a Synthetic Case

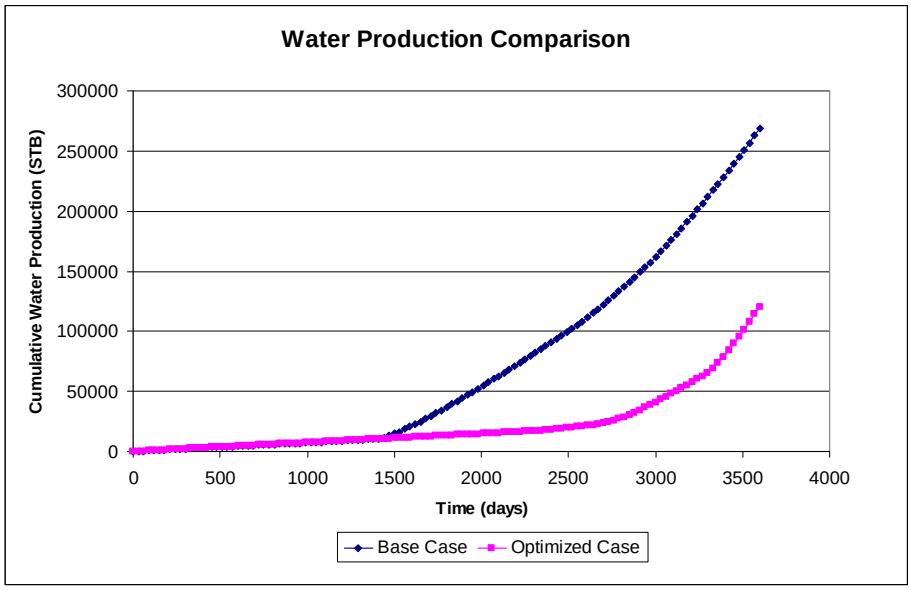

Figure 3.5 Comparison of Water Production Profiles of a Synthetic Case

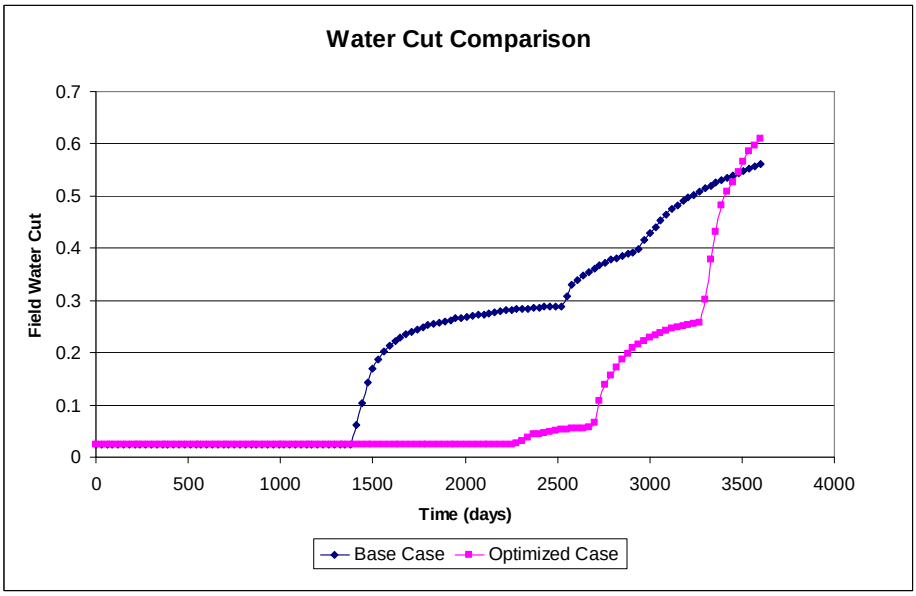

Figure 3.6 Comparison of Water Cut Profiles of a Synthetic Case

We also conducted the optimization scheme on multiple realizations to account for the geological uncertainty. The permeability fields of nine realizations are shown in Figure 3.7, which reveal a northwest to southeast trend. After the arrival time optimization scheme is conducted, the optimized results are shown from Figures 3.8 to 3.10.

The objective function of multiple realizations case is formulated as the expected value of that from individual realizations. While optimizing the oil production and sweep efficiency in the field, it also takes into account the geological uncertainty. From the figures, the optimized results for multiple realizations are between the base case and the single realization case. The conservativeness of the results shows its consideration of the uncertainty in the field.

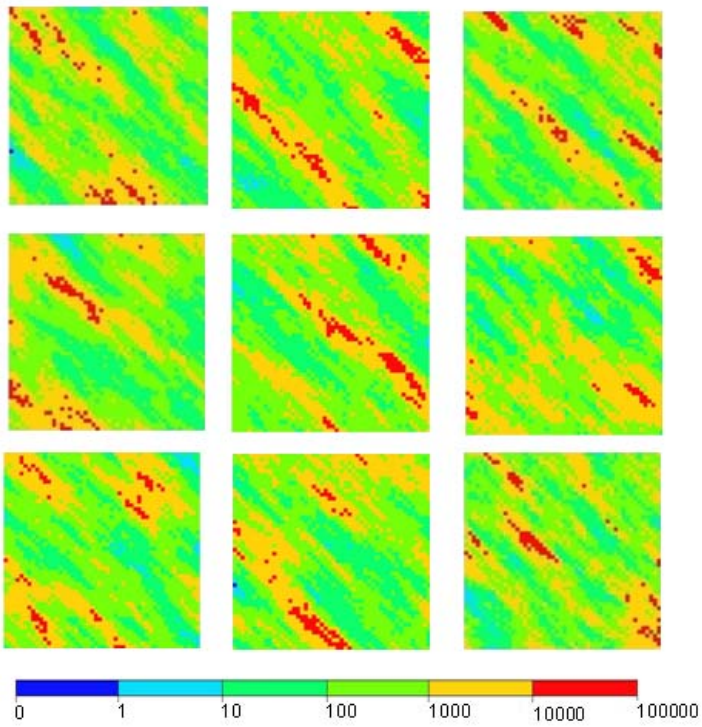

Figure 3.7 Permeability Fields of Multiple Realizations

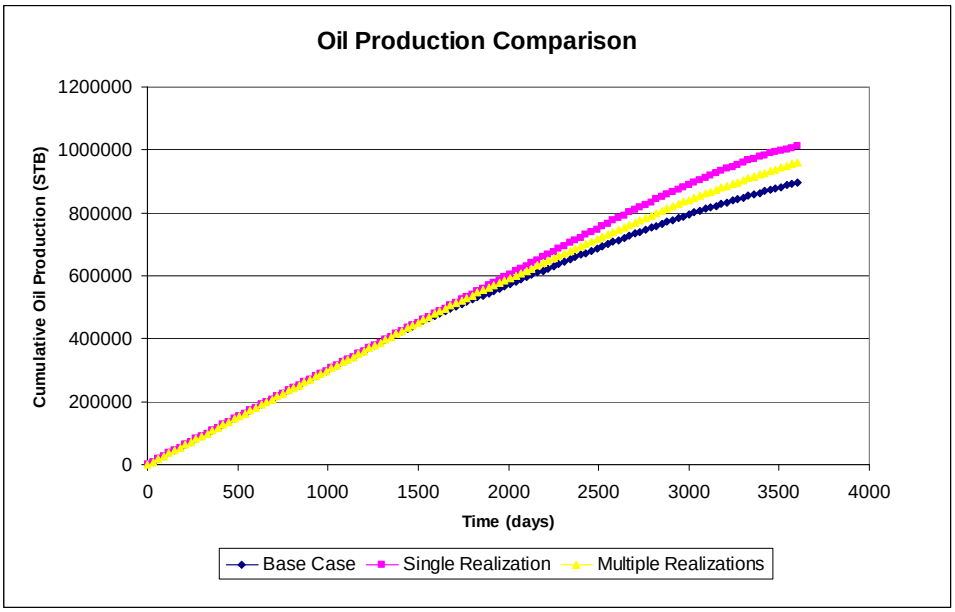

Figure 3.8 Comparison of Oil Production Profiles of Brugge Field

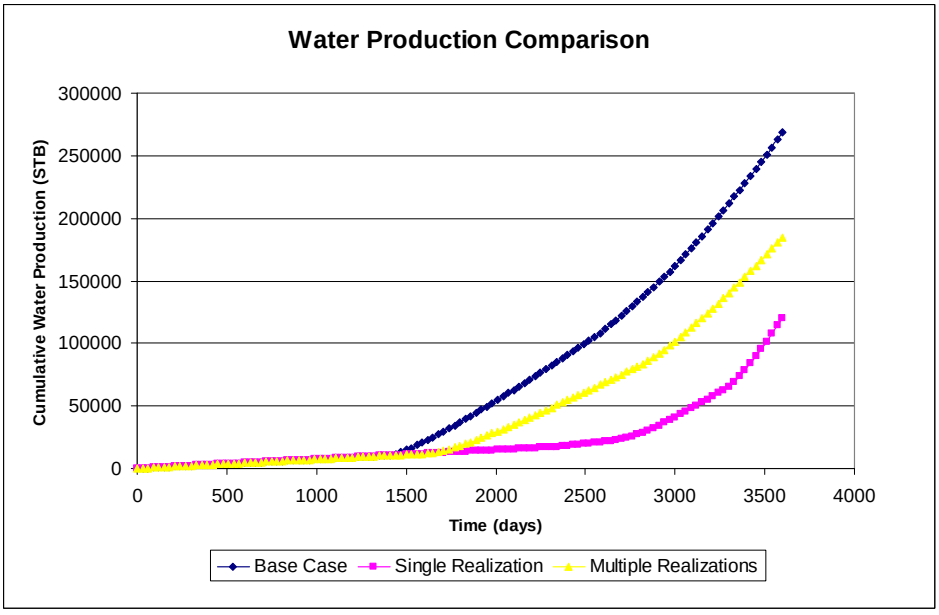

Figure 3.9 Comparison of Water Production Profiles of Brugge Field

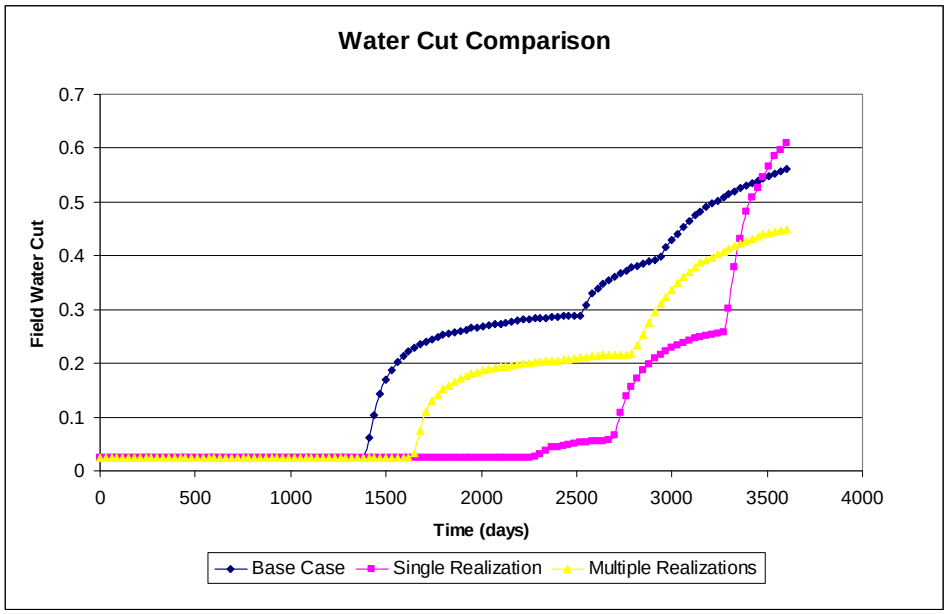

Figure 3.10 Comparison of Field Water Cut Profiles of Brugge Field

3.2 Brugge Field Case

In this section we will conduct the arrival time optimization approach on the Brugge field over 20 years. The Brugge field is a synthetic benchmark case that was set up by TNO as part of an SPE ATW to evaluate various closed loop control strategies. The details for this case can be found in Peters et al. (2009).

A series of model realizations were generated based on reservoir properties and well log attributes extracted from a highly-resolution model consisting of 20 million grid cells. The Brugge field properties are based on a North Sea Brent-type field. The structure of the Brugge field consists of an E-W elongated half-dome with a large boundary fault at its north edge, and one internal fault with a modest throw at an angle of around 20 degrees to the north boundary fault. The model consists of 60000 gridblocks

with 9 layers. It has 20 vertical producers completed mainly in the top 8 layers and 10 peripheral injectors completed in all 9 layers. The field structure and well locations are shown in Figure 3.11.

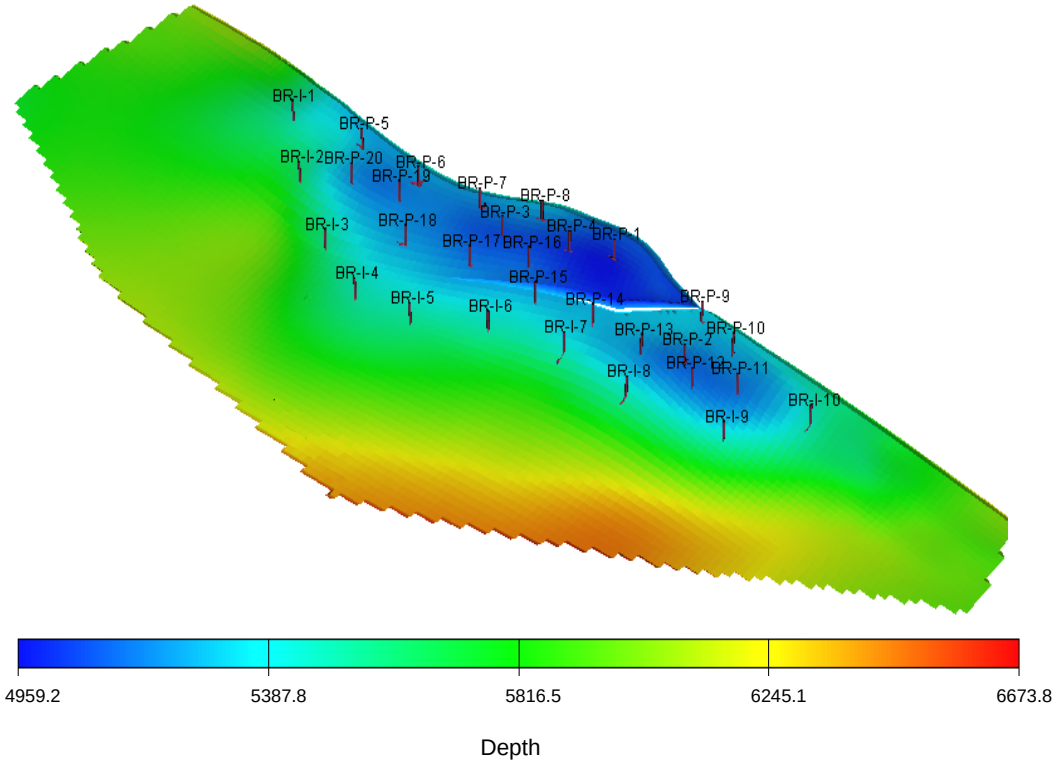

Figure 3.11 Map Showing the Structure of Brugge Field and Wells Locations

The first 10 years of the production history of the field was provided for history matching purposes. The production history was based on a 'true model' response with added noise. The closed loop control approach consisted of two steps: (i) model updating via production data integration using the field production history for the first 10 years and (ii) production optimization whereby rates are allocated over the next 20 years.

In our study, we only consider the production optimization part on Brugge field. We assume history matching result is provided. The optimization is performed to improve sweep efficiency over single history matched model by equalizing the arrival times at the producers. For optimization purposes, we divided the wells into two groups based on the location of the internal fault. Group 1 includes the following producing wells: BR-P-1, 3, 4, 5, 6, 7, 8, 16, 17, 18, 19, 20 and the following injection wells: BR-I-1, 2, 3, 4, 5, and 6. Group 2 has the following producing wells: BR-P-2, 9, 10, 11, 12, 13, 14, and 15, and the following injection wells: BR-I-7, 8, 9, and 10.

Most of the wells are equipped with three inflow control valves (ICVs). We consider two production scenarios: (i) using original wells for production optimization and (ii) controlling the rates of ICVs for optimization.

The additional constraints imposed are as follows,

- The maximum production rate per producer is 3000 rb/Day.
- The maximum Injection rate per injector is 4000 rb/Day.
- Maximum allowable flowing bottom-hole pressure is 2626 psia.
- The minimum allowable flowing bottom-hole pressure is 740 psia.
- The optimized rates are reported at each ½ a year.

We have preformed the optimization under two scenarios. The first one using original wells imposes voidage replacement constraint and maintains the reservoir pressure. To accomplish this, we imposed the constraint that the injection for each well group is equal to the total production from the same group. In addition, any production wells with water cut exceeding 90% will be shut in. In the second scenario, we use ICVs

instead of original wells. Additionally, we do not keep voidage balance and attempt to produce the field at its maximum allowable production rate (60000 RB/D). The production here falls off gradually because of well bottom hole pressure constraints and water cut constraints. The total injection for this case is constrained to 40000 RB/D for the whole optimization period. Any production ICVs with water cut exceeding 90% will be shut in.

Figures 3.12 to 3.14 show a comparison between the base case and the optimized cases for both scenarios in terms of cumulative oil production and water production. The results indicate an increase in oil production and a substantial decrease in water production for both scenarios. As we discussed earlier, our optimization approach attempts to maximize the sweep efficiency. This is demonstrated in Figure 3.15 which compares the oil saturation maps for the top three layers between the base case and the optimized cases for both scenarios. The results indicate improved sweep for the optimized cases over the base case as indicated by circles.

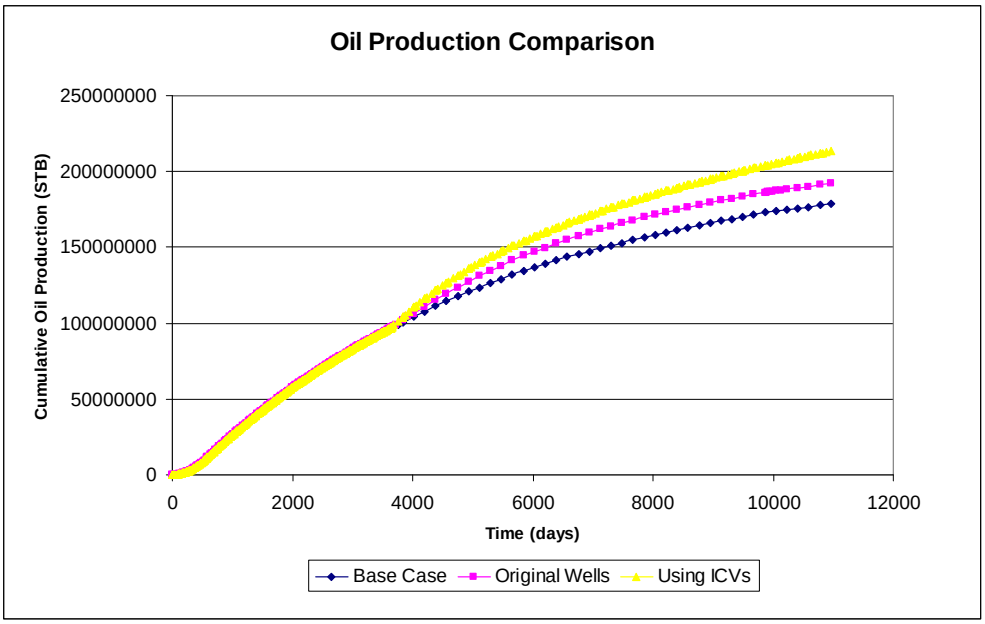

Figure 3.12 Oil Production Profiles of Brugge Field

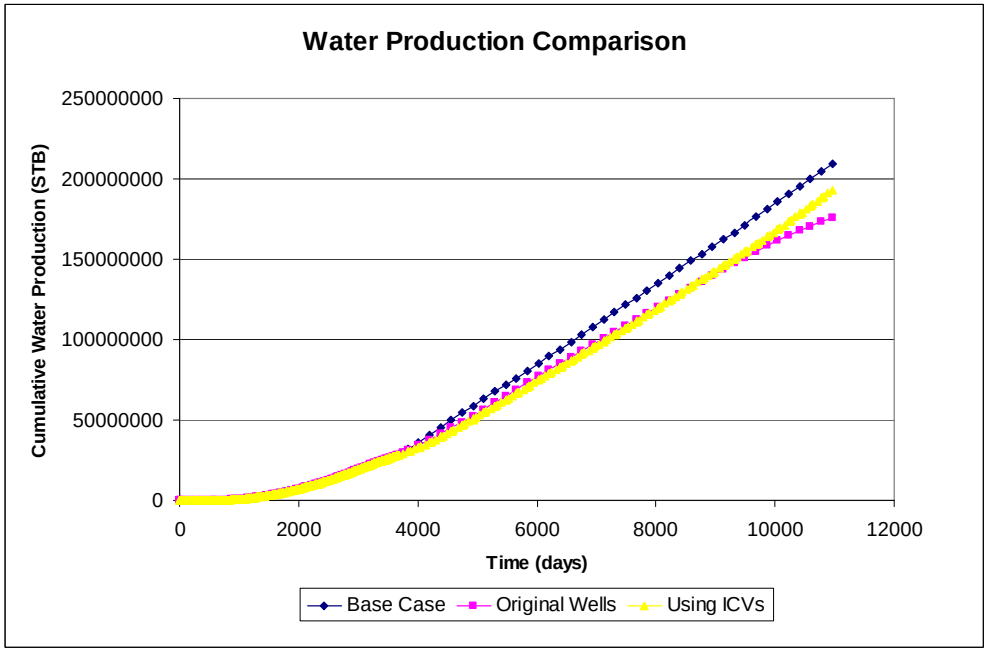

Figure 3.13 Water Production Profiles of Brugge Field

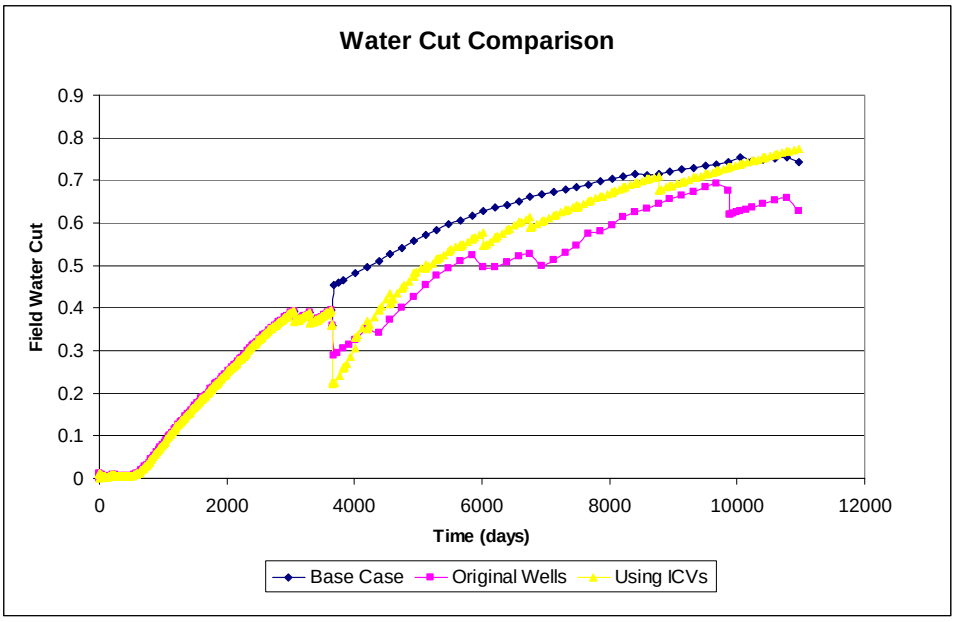

Figure 3.14 Water Cut Profiles of Brugge Field

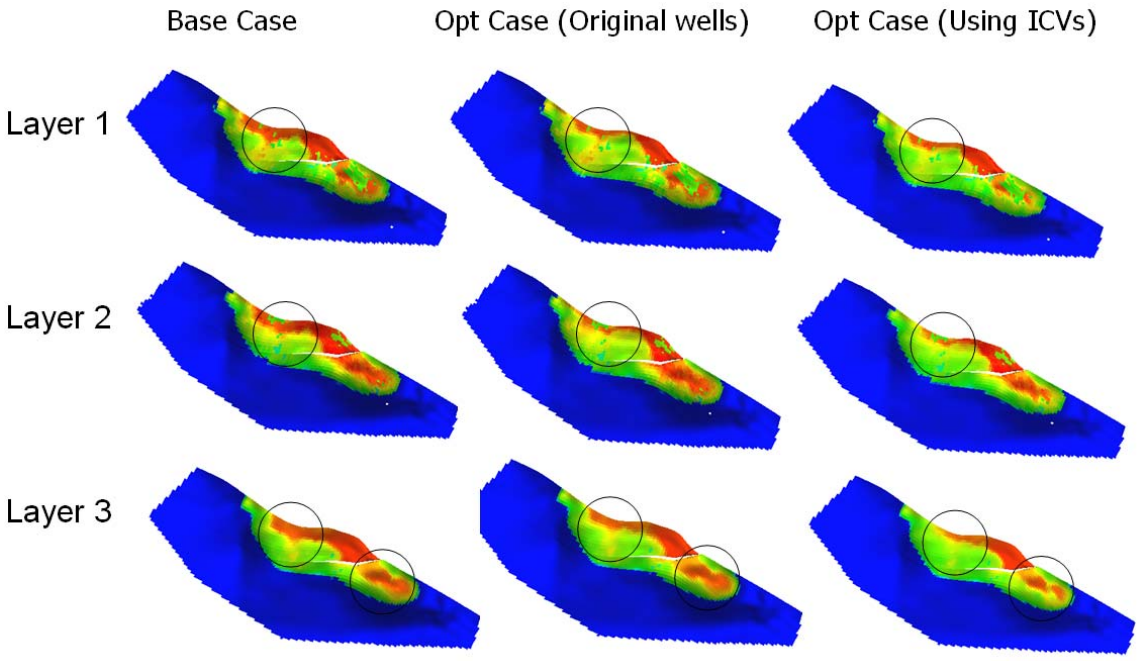

Figure 3.15 Oil Saturation Maps of Top Three Layers

Comparing the two production scenarios, the second scenario using ICVs and no voidage balance shows a higher cumulative oil production in Figure 3.12, and thus gives a higher net present value. Figures 3.16 and 3.17 show a comparison between both scenarios in terms of reservoir pressure and total production. The total injection rate is the same for both scenarios and is equal to 40000 RB/D for the whole period as mentioned earlier. The reservoir pressure for the first scenario is maintained at its initial level because the production/injection ratio is kept close to unity and the reservoir fluids are nearly incompressible. The reservoir pressure for the second scenario falls off sharply at the beginning because the production/injection ratio is greater than 1 to start with and then the pressure levels off when the production/injection ratio becomes nearly 1.

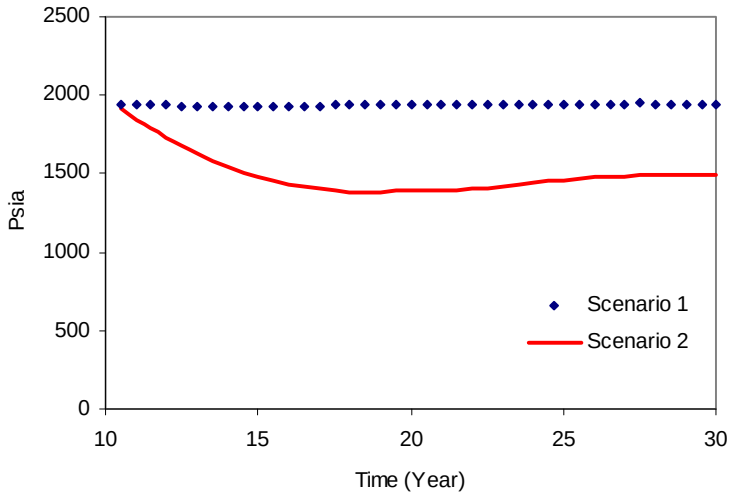

Figure 3.16 Reservoir Pressure between Two Production Scenarios

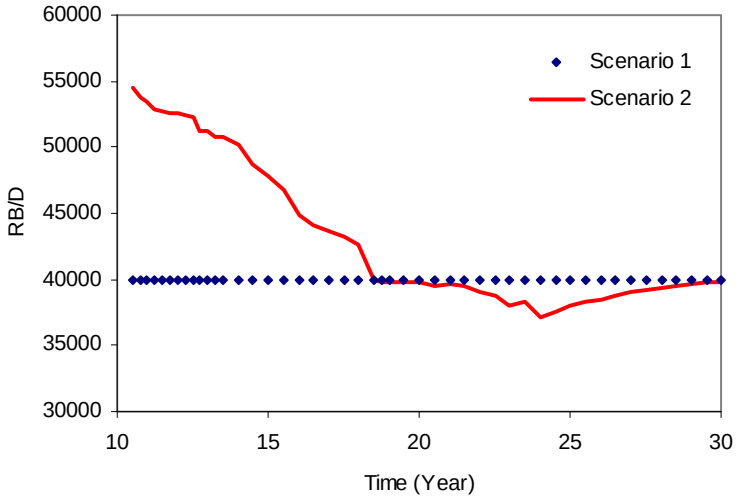

Figure 3.17 Total Field Production Rate between Two Production Scenarios

4. COMPARISON BETWEEN ARRIVAL TIME OPTIMIZATION AND NPV OPTIMIZATION

In this section, we will compare the two optimization schemes: arrival time optimization and NPV optimization. After showing the limitations of the arrival time optimization, we will introduce the accelerated arrival time optimization which has an acceleration term in the objective function.

4.1 Reservoir Description

The comparison is based on a 4-spot synthetic case. The permeability field and well locations are shown in Figure 4.1. Well P1 is located in the high permeability streak, which will lead to early water breakthrough for the well. Well P2 is in the low permeability area, so it will have the latest water breakthrough. For Well P3, it should have a water breakthrough earlier than P2 but later than P1. The total production time is 5000 days. For NPV calculation, we set the oil price as 50$/bbl, water disposal price 5$/bbl, discount rate 10%.

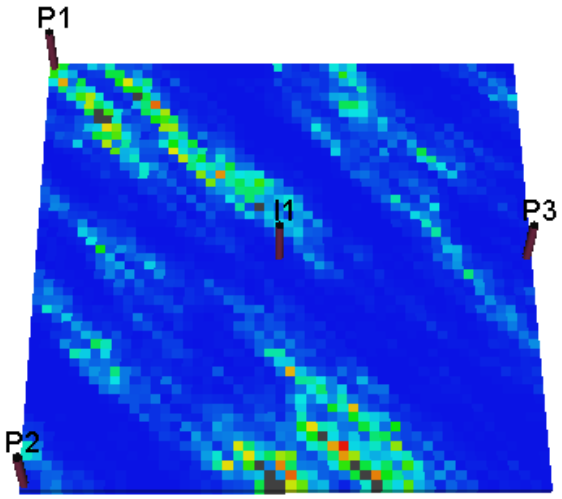

Figure 4.1 Permeability Field and Well Configuration

4.2 Comparison Based on Single Time Step

First we conduct both optimization schemes on this example using only one time step. In other words, the initial control will last for the whole production period. Equality constraints are imposed in this case: total production rate = injection rate = 400 rb/d and voidage balance is maintained. As discussed in Section 2, the NPV optimization will use perturbation method to calculate the gradients numerically.

By changing the production rates of Well P1 and P2, we can plot the contour maps of objective functions for both arrival time optimization and NPV optimization. Figures 4.2 and 4.3 show the contours in the vicinity areas of the peak values in terms of the maximum NPV and minimum arrival time misfit respectively. The maximum NPV area generally matches the minimum arrival time misfit area. Table 4.1 shows the

optimal rates generated by both optimization methods. Comparing these two optimal values, we find that they are almost identical.

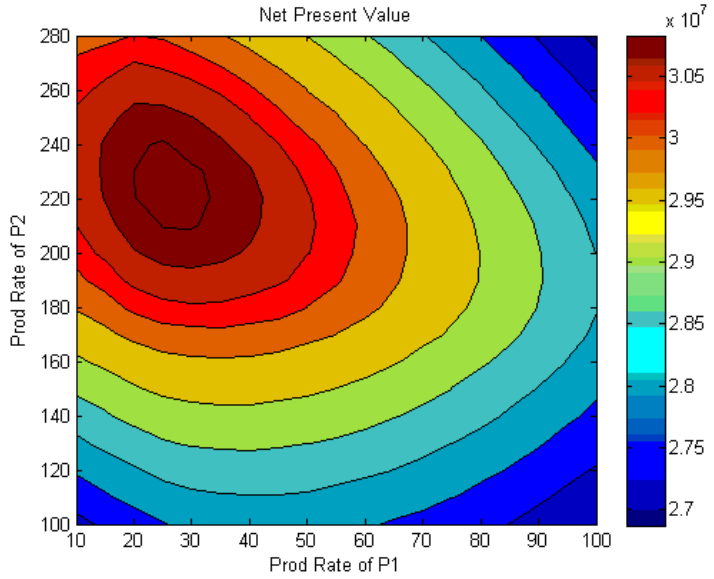

Figure 4.2 Contour Map of Net Present Value

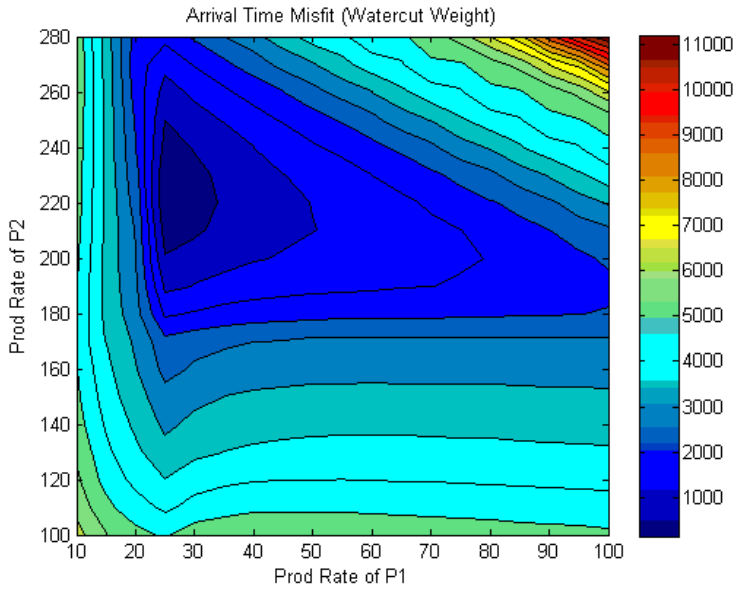

Figure 4.3 Contour Map of Arrival Time Misfit

Table 4.1 Optimal Rates Comparison

	NPV Optimization	Arrival time optimization
P1	25.6966	25.5496
P2	225.498	224.0731
P3	148.8154	150.3775

We also plot the contour map for the accelerated arrival time misfit in Figure 4.4. In this new objective function, it not only contains the misfit term, but also has the arrival time norm penalty term for acceleration purposes. The optimization algorithm will minimize both the arrival time and its misfit, so that the production strategy will consider accelerating the production as well as field sweep efficiency.

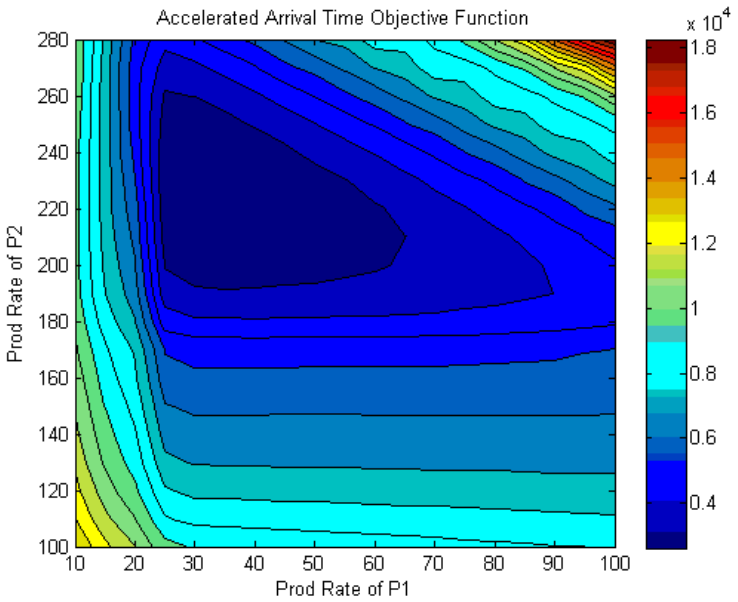

Figure 4.4 Contour Map of Accelerated Arrival Time Misfit

4.3 Comparison Based on Multiple Time Steps

4.3.1 Equality Constraint

The comparison of arrival time optimization and NPV optimization is conducted on the synthetic case using five time steps, with equal time step size of 1000 days. Equality constraint is imposed: total production rate = 800 rb/d, and the voidage balance is kept by maintaining injection rates equal to total production rate. Upper boundary of well rate is 300 rb/d, while lower boundary is 10 rb/d.

Table 4.2 shows the optimal rates for NPV optimization, while Table 4.3 shows the optimal rates for arrival time optimization. Their rate allocations are different. Figure 4.5 shows the oil saturation map comparison between these two optimizations. The arrival time optimization gives a more uniform water front movement as shown in those areas pointed by circles. Table 4.4 shows the NPV comparisons. The NPV generated by arrival time optimization is close to that of NPV optimization. Figure 4.6 shows the objective function behaviors through iterations for these two optimizations. Both of them converge smoothly.

Table 4.2 Optimal Rates of NPV Optimization for Equality Constraint Case

	Step 1	Step 2	Step 3	Step 4	Step 5
P1	271.0919	19.56815	16.62727	10	10
P2	90.64117	135.3258	222.6537	288.4016	144.3805
P3	38.26697	245.1061	160.719	101.5984	245.6195

Table 4.3 Optimal Rates of Arrival Time Optimization

	Step 1	Step 2	Step 3	Step 4	Step 5
P1	36.2955	37.3304	36.5883	24.71	19.828
P2	218.8016	217.5585	215.1828	258.8684	217.1384
P3	144.9031	145.111	148.2287	116.4215	163.0337

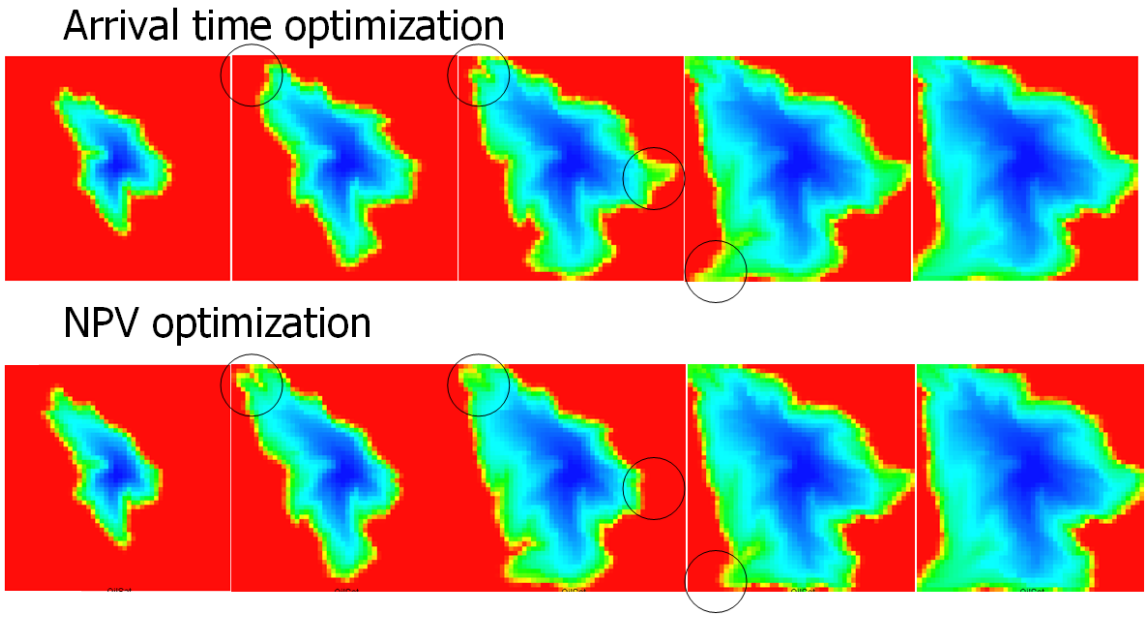

Figure 4.5 Oil Saturation Maps Comparison

Table 4.4 NPV Comparison for Equality Constraint Case

	NPV
NPV Optimization	4.129E+07
Arrival Time Optimization	4.094E+07

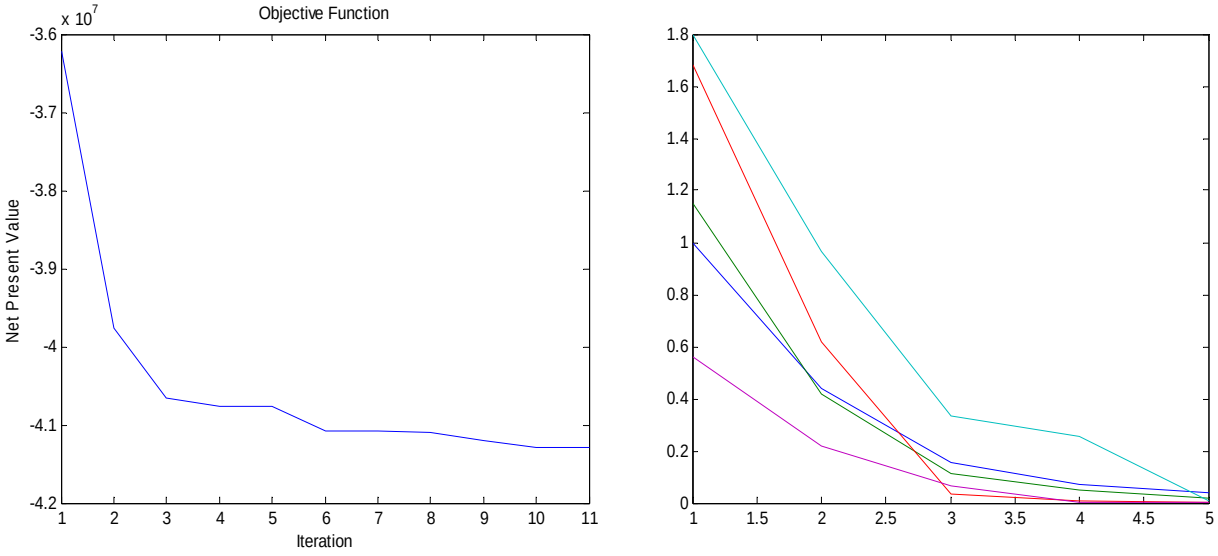

NPV Optimization Arrival Time Optimization

Figure 4.6 Objective Function Behaviors

4.3.2 Inequality Constraint

Sometimes we do not know how much total production rate we should keep. So, for this case we use the inequality constraint: total production rate ≤ 800 rb/d. We still keep the other specifications: five time steps and voidage balance constraint, as well as the same upper and lower boundaries of well rates.

Table 4.5 shows the optimal rates of arrival time optimization. Table 4.6 shows the optimal rates of NPV optimization. The optimal rates of arrival time optimization are much lower than those of NPV optimization since the objective function does not have any acceleration factor. From Table 4.7, the arrival time optimization gives an optimal NPV as 4.531E+07, which is much lower than that of the NPV optimization 5.778E+07.

Table 4.5 Optimal Rates of Arrival Time Optimization with No Acceleration

	Step 1	Step 2	Step 3	Step 4	Step 5
P1	40.7599	43.7839	43.2248	23.3317	28.183
P2	235.0177	240.4057	286.5765	291.7489	259.5953
P3	159.056	163.404	165.7406	188.1575	259.5574
Total	434.8335	447.5937	495.5417	503.2379	547.3357

Table 4.6 Optimal Rates of NPV Optimization for Inequality Constraint Case

	Step 1	Step 2	Step 3	Step 4	Step 5
P1	199.948	158.5967	10	10.0406	39.5141
P2	300	300	300	300	300
P3	300	300	300	300	299.99
Total	799.948	758.5967	610	610.0406	639.5041

Table 4.7 NPV Comparison for Inequality Constraint Case

	NPV
Arrival Time Optimization	4.531E+07
NPV Optimization	5.778E+07
Accelerated Arrival Time Optimization	5.727E+07

However, the accelerated arrival time optimization can counteract the deficiency in terms of NPV and deliver an optimal result which will give good NPV as well as sweep efficiency. Table 4.8 shows the optimal rates from the accelerated arrival time optimization. It has high rates at early production period to account for the discount rate. The optimal NPV is 5.727E+07 as shown in Table 4.7, which is very close to that of the NPV optimization.

Table 4.8 Optimal Rates of Accelerated Arrival Time Optimization

	Step 1	Step 2	Step 3	Step 4	Step 5
P1	200.0646	200.0615	10.0717	12.8019	10
P2	299.2835	299.284	299.2842	288.55	208.2634
P3	299.2847	299.2852	299.2853	287.2761	208.3485
Total	798.6325	798.6308	608.6406	588.628	426.6119

Figures 4.7 and 4.8 show the contour maps of the NPV and accelerated arrival time misfit in the vicinity of the solution. They have the same general peak value areas and convergence trends.

Figure 4.9 shows the comparison of the oil saturation maps at the middle and the end of production period between arrival time optimization, NPV optimization and accelerated arrival time optimization. The arrival time optimization with acceleration has swept the field much better than that with no acceleration and its oil saturation map is similar to that of NPV optimization.

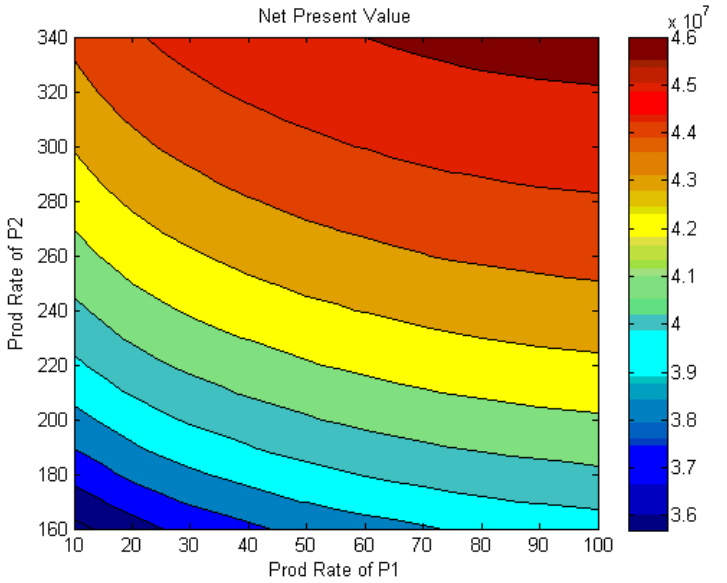

Figure 4.7 Contour Map of Net Present Value

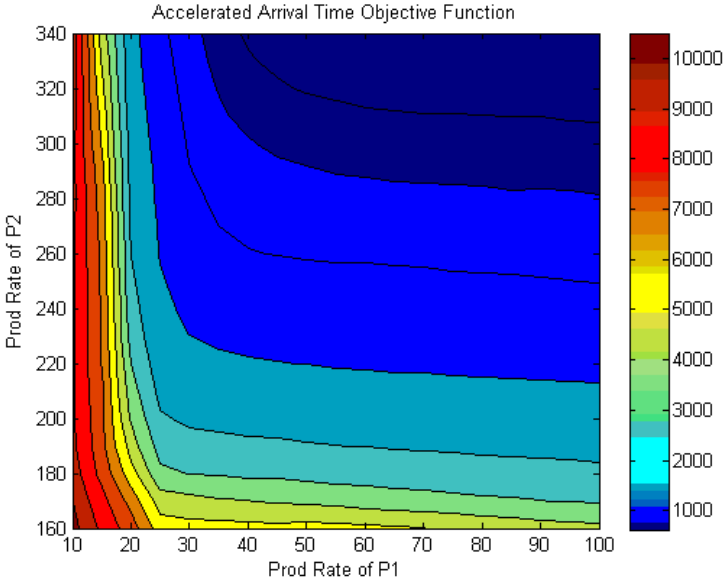

Figure 4.8 Contour Map of Accelerated Arrival Time Misfit

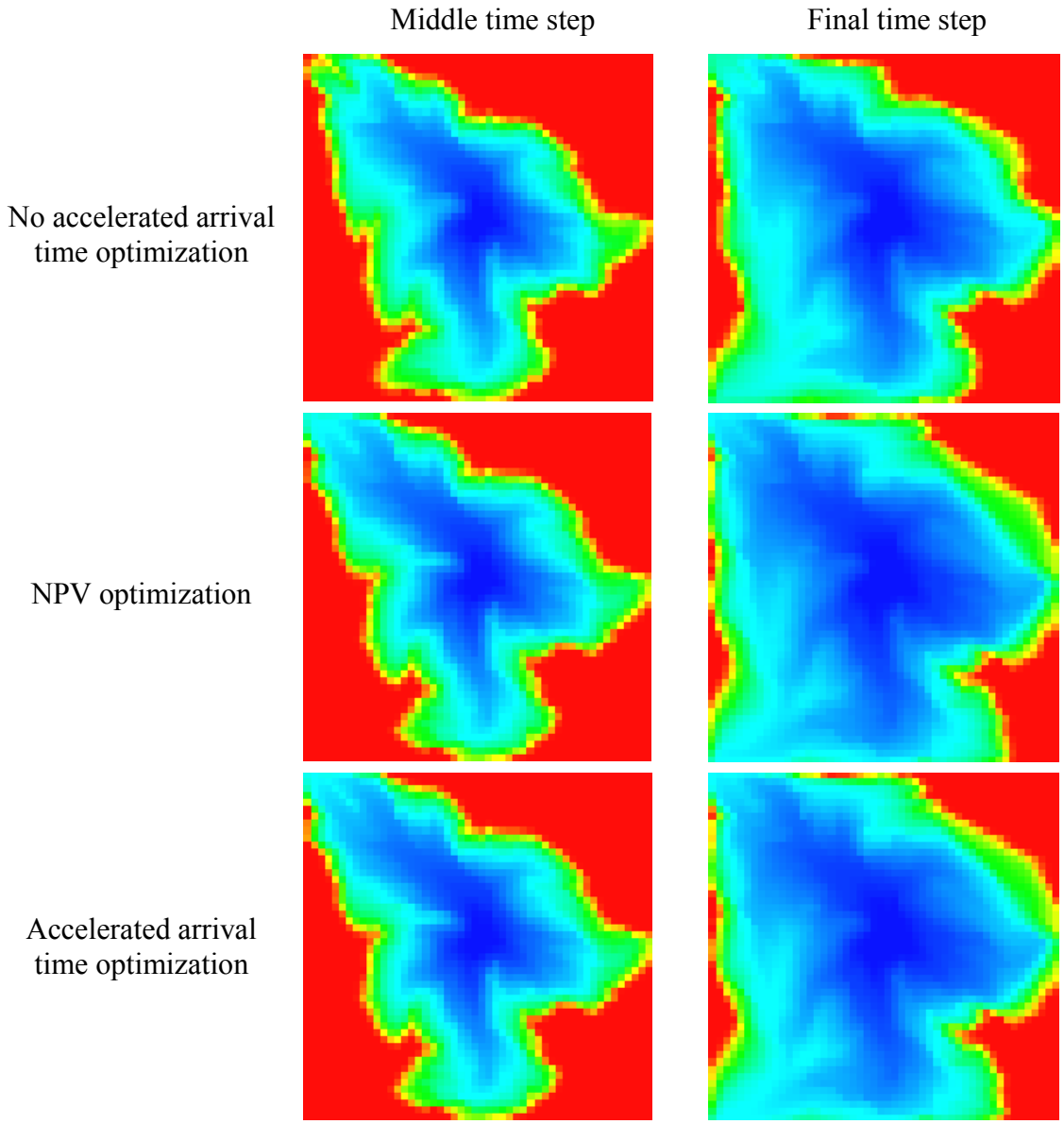

Figure 4.9 Comparison of Oil Saturation Maps between Arrival Time, NPV and Accelerated Arrival Time Optimization

Figure 4.10 shows the oil production profile between the NPV optimization and accelerated arrival time optimization. Their oil production profiles are almost identical. We also plot oil recovery versus water injection in Figure 4.11, the trends of the plots between NPV optimization and accelerated arrival time optimization overlap.

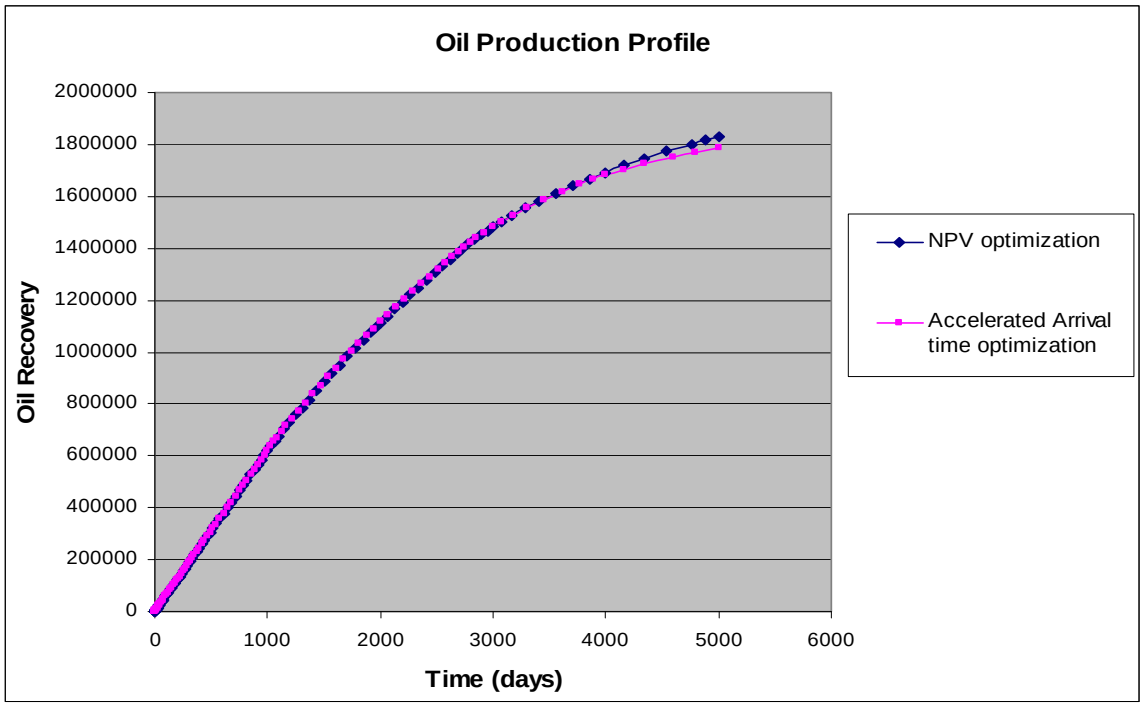

Figure 4.10 Oil Production Profile of NPV Optimization and Accelerated Arrival Time Optimization

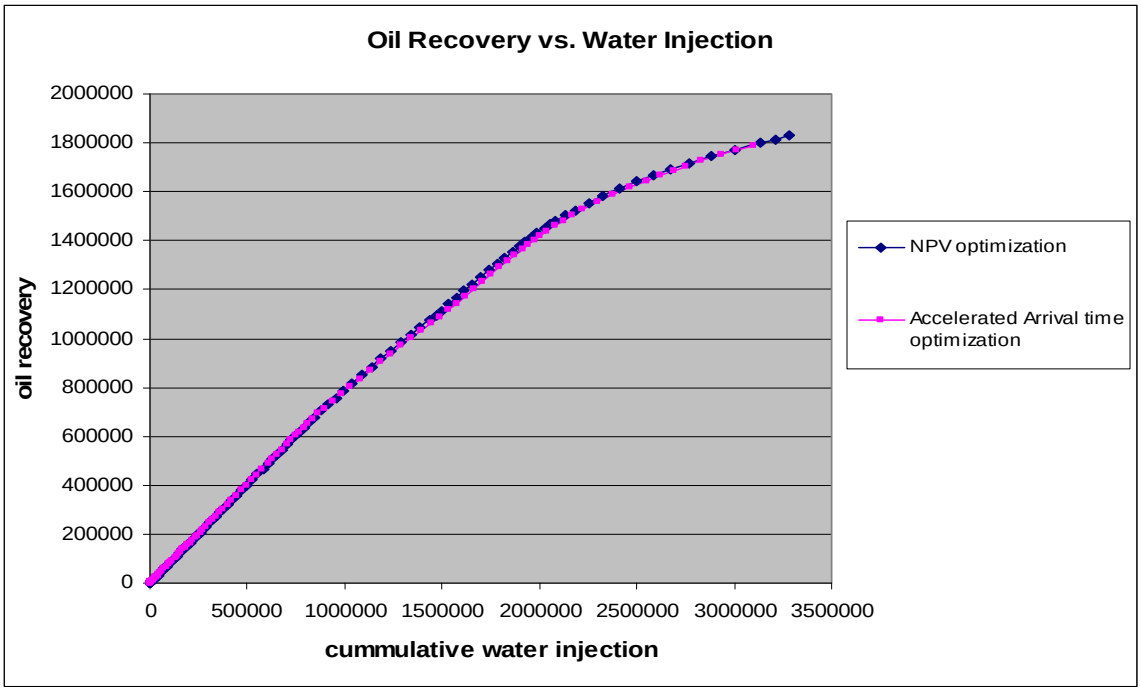

Figure 4.11 Oil Recovery vs. Water Injection

4.4 Weighting Factor

In the formulation of the accelerated arrival time optimization, we need to consider a weighting factor between the two terms: arrival time and its misfit. We plot the NPV with respect to the weight on acceleration term in Figure 4.12. The NPV increases with the weighting factor initially and then it reaches a plateau where it remains the same amount. In this case, the plateau starts from weighting factor 0.8 as shown in the figure. We use weighting factor as 1 in our previous comparison.

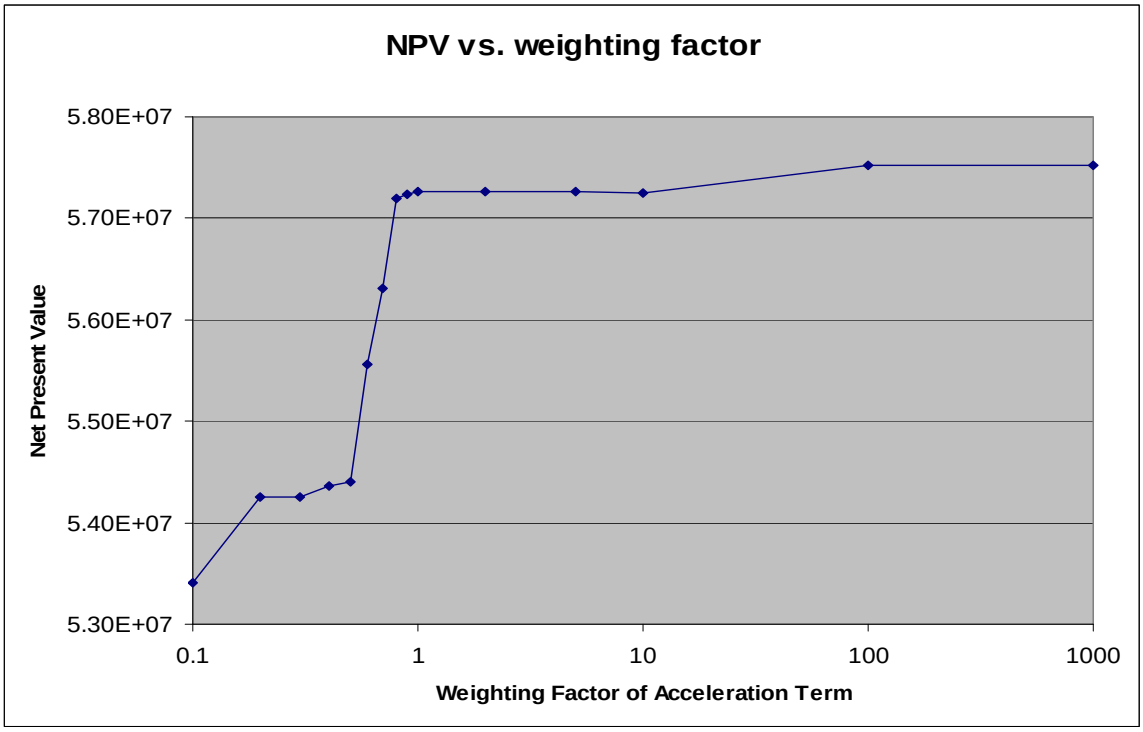

Figure 4.12 NPV Profile with Respect to Weighting Factor of Acceleration Term

To illustrate the effect of the weighting factor on the optimization process, we run another case with weighting factor equal to 0.7. The optimal rates generated from the accelerated arrival time optimization is in Table 4.9.

Table 4.9 Optimal Rates of Accelerated Arrival Time Optimization (weighting factor = 0.7)

	Step 1	Step 2	Step 3	Step 4	Step 5
P1	117.8117	200.0627	10.0705	13.5411	17.5831
P2	299.2835	299.2838	299.2841	288.5489	288.4786
P3	299.2847	299.285	299.2852	262.2508	266.0802
Total	716.3796	798.6312	608.6398	564.3408	572.142

The optimal net present value with weighting factor 0.7 is 5.631E+07, which is lower than the NPV of the optimization with weighting factor 1.

Figure 4.13 shows the oil saturation map comparison between NPV optimization, accelerated arrival time optimization with weighting factors 0.7 and 1.

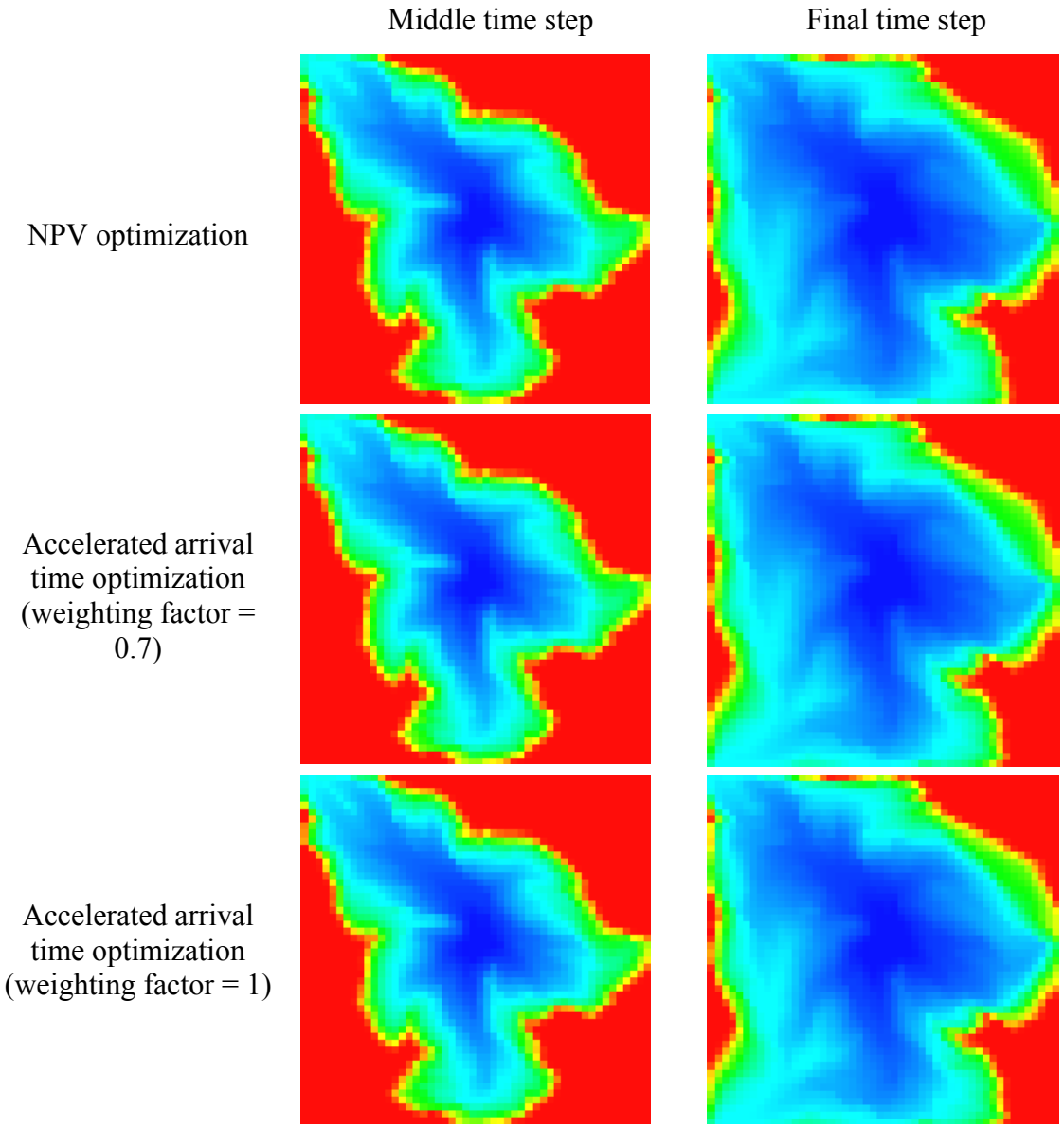

Figure 4.13 Comparison of Oil Saturation Maps with Different Weighting Factors

Figure 4.14 shows the oil production profiles in four control scenarios: NPV optimization with discount rate, without discount rate and accelerated arrival time optimization with weighting factor 0.7 and 1.

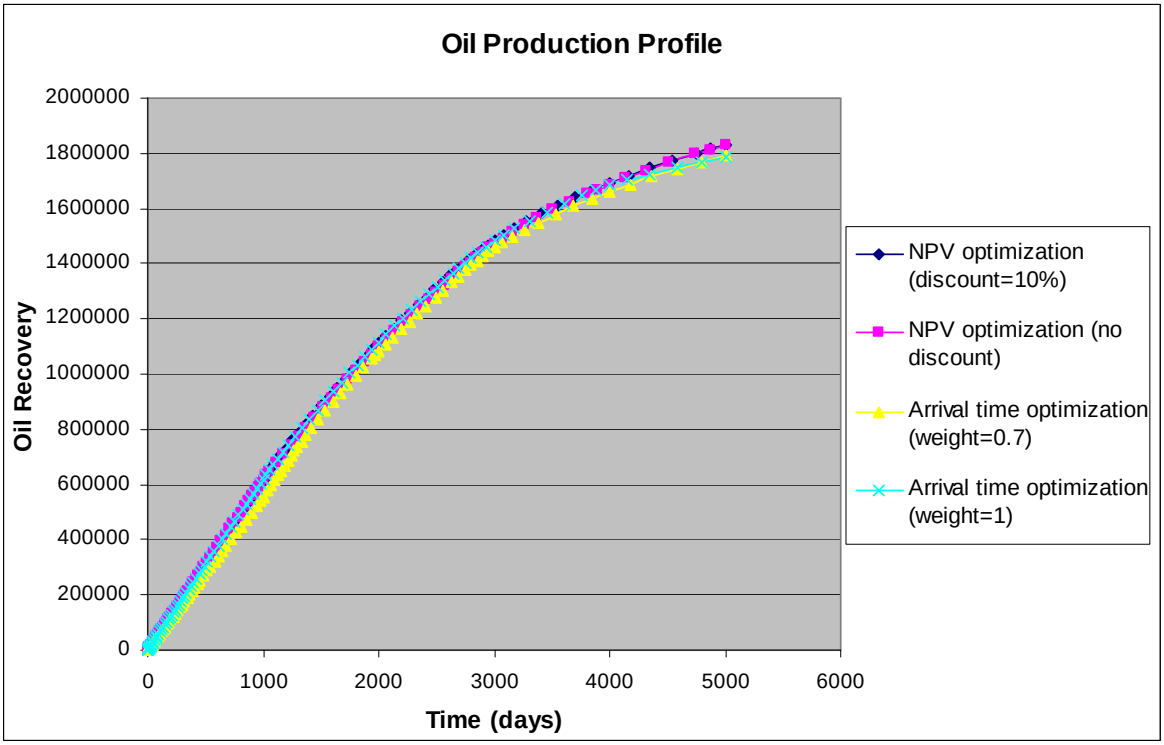

Figure 4.14 Comparison of Oil Production Profiles between NPV and Accelerated Arrival Time Optimization

Figure 4.15 shows the oil recovery versus water injection profiles for those four control scenarios: NPV optimization with discount rate, without discount rate and accelerated arrival time optimization with weighting factor 0.7 and 1.

The oil production profiles and oil recovery versus water injection profiles show the capability of the accelerate arrival time optimization to achieve a good oil recovery.

The weighting factor is an adjustable parameter and it will have certain impact on the optimization results. In this case, the arrival time optimization with weight equal to 1 performs better than that of weight equal to 0.7 in terms of oil production.

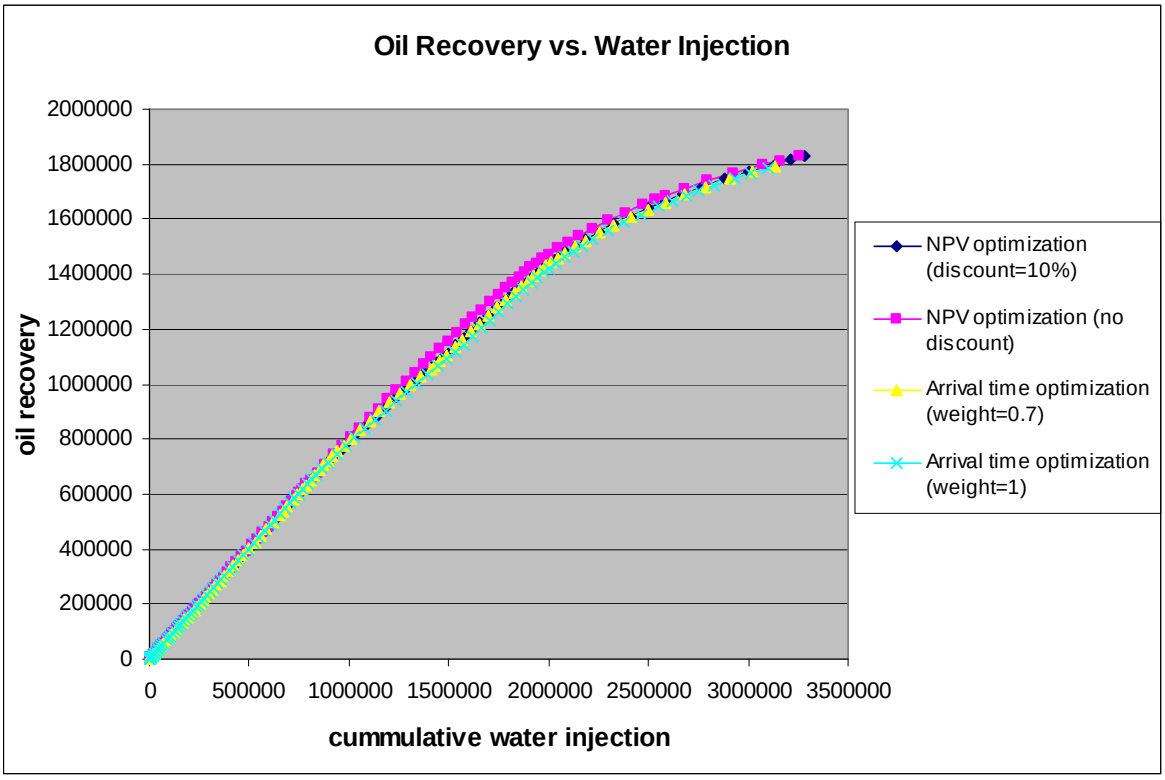

Figure 4.15 Comparison of Oil Recovery vs. Water Injection between NPV and Accelerated Arrival Time Optimization

5. CONCLUSIONS AND RECOMMENDATIONS

5.1 Conclusions

Field scale rate optimization problems often involve highly complex reservoir models, production and facilities related constraints and a large number of unknowns. The primary objective of arrival time optimization algorithm is to enhance the sweep efficiency in a waterflood project by equalizing the arrival times of the water front at multiple producers and correspondingly increasing the cumulative oil production. The arrival time optimization uses streamlines to efficiently and analytically compute the sensitivity of the arrival times with respect to well rates. It can account for geologic uncertainty via a stochastic framework that relies on a combination of the expected value of the objective functions from multiple realizations. The gradients and Hessian of the objective function can be calculated analytically which makes the optimization computationally efficient for large field cases. The optimization is performed under operational and facility constraints using a sequential quadratic programming approach. The optimization is performed at multiple time steps to account for mobility effects, changing field conditions and non-linear constraints. This approached is implemented using finite difference simulators to extend the scope for future study.

The arrival time optimization has been compared with NPV optimization. The NPV optimization focuses on the economic side of field production, while the arrival time optimization is trying to maximize the field sweep efficiency. Both methods have shown to improve the oil recovery and delay the water production in the field. In order to counteract the limitations of arrival time optimization that it may not be able to

accelerate the field oil production, we add a regularization term in the objective function of arrival time optimization to accelerate the oil production. The results have shown that the accelerated arrival time optimization can maximize the sweep efficiency while giving a comparable net present value to that of NPV optimization. One thing we need to consider about the acceleration term is its weighting factor. The weighting factor needs to be adjusted to provide the optimal control strategy. Our new technique is trying to find the optimal balance between NPV and sweep efficiency in the field.

5.2 Recommendations

Several recommendations that could improve the performance of the arrival time optimization algorithm or extend the comparison between arrival time and NPV optimization are listed below:

1. Further investigation needs to done to address a general rule to determine the optimal value of the weighting factor in the objective function of accelerated arrival time optimization. It is hard to address the value analytically since it is a highly nonlinear problem. We may try to update the weight after each iteration instead of keeping it constant during the whole optimization process. By updating the weight, we can obtain the appropriate compromise of the relative weight between the two terms in the objective function and achieve the best control strategy.
2. After the arrival time optimization is implemented using finite difference simulators, we can extend the optimization scope to compositional flows. Finite

difference simulators are more mature in compositional flow simulation and thus if we have a streamline tracing post processor that can handle compositional flows, we will be able to further our optimization study in more complicated fields.

3. The comparison between NPV optimization and arrival time optimization is conducted on a synthetic case in our study. Further study could involve the comparison on other kinds of cases, such as channelized cases or field cases. The number of control variables might be increased on a more complicated case, and thus, the computation would be more expensive. It might be necessary to implement more efficient gradient calculation method to substitute for perturbation method, for example, the adjoint gradients, so that the comparison could be applied on a large field case.

NOMENCLATURE

A	area along the streamline, sp ft [m^2]
A	matrix contains linear operators
b	discount rate
B_o	oil FVF, STB/bbl [stock-tank m^3/m^3]
B_w	water FVF, STB/bbl [stock-tank m^3/m^3]
b	vector contains constant elements
C	matrix contains linear operators
$f(\mathbf{q})$	scalar objective function, sq day
f_w	fractional flow, dimensionless
e	arrival time residual vector, day [s]
$e_{i,m}$	arrival time residual at well *i* (producer) which belong to group *m*, day [s]
g(q)	inequality constrains
h(q)	equality constrains
I	identity matrix
i and *j*	well index
k	permeability, darcies
J	Jacobian matrix
m	group index
$N_{prod,m}$	number of production wells in group *m*
N_{group}	number of groups
$N_{sl,I}$	number of streamline connecter to well *I* (producer)

$N_{fsl,i}$	number of fast streamlines connected to well *i* (producer)
$N_{fsl,i,j}$	number of fast streamlines between well *i* (producer) and well *j* (injector)
l	streamline index
P_i	initial pressure, psi [kPa]
P_b	grid block pressure, psi [kg/m^2]
P_r	reservoir pressure, psi [kg/m^2]
P_{wf}	well's flowing bottom hole pressure psi [kg/m^2]
$\mathbf{q}$	total fluid rate vector, B/D [m^3/d]
q	total fluid rate B/D [m^3/d]
q_{sl}	total fluid rate along a single streamline, B/D [m^3/d]
r	risk coefficient, dimensionless
r_o	oil price, $/bbl
r_{wp}	water price for production, $/bbl
r_{wi}	water price for injection, $/bbl
$\partial\mathbf{R}$	vector of change in reservoir property
s_w	water saturation, fraction
s_{wf}	flood-front saturation, fraction
$s(\mathbf{x})$	slowness, day [s]
$\mathbf{S}$	sensitivity matrix, sq D/B [s^2/ m^3]
$S_{i,j}$	sensitivities coefficient, sq D/B [s^2/ m^3]
$t_{i,m}$	arrival time at producer *i* which belongs to group *m*, day [s]
$t_{d,m}$	desired arrival time for group *m*, day [s]

v	velocity, ft/D [m/d]
w	weight, dimensionless
x	spatial coordinate vector, ft [m]
x	distance along the streamline, ft [m]
y	number of inequality constraints
z	number of equality constraints
$\boldsymbol{\lambda}_L$	Lagrange multipliers for equality constraints
$\boldsymbol{\lambda}_K$	Karush-Kuhn-Tucker multipliers for inequality constraints
β	weighting factor
μ_o	oil viscosity, cp [Pa • s]
μ_w	water viscosity, cp [Pa • s]
ρ_o	water viscosity, lbm/cu ft [kg/m^3]
ρ_w	water viscosity, lbm/cu ft [kg/m^3]
ϕ	porosity, fraction
σ	standard deviation

REFERENCES

Alhuthali, A.H., Oyerinde, D., and Datta-Gupta, A. 2007. Optimal Waterflood Management Using Rate Control. *SPEREE* **10** (5): 539-551. SPE: 102478-PA. DOI: 10.2118/102478-PA.

Alhuthali, A.H., Datta-Gupta, A., Yuen, B, and Fontanilla, J.P. 2008. Optimal Rate Control Under Geologic Uncertainty. Paper SPE 113628 presented at the SPE/DOE Symposium on Improved Oil Recovery, Tulsa, Oklahoma, 20-23 April. DOI: 10.2118/113628-MS.

Alhuthali, A.H., Datta-Gupta, A., Yuen, B, and Fontanilla, J.P. 2009. Field Applications of Waterflood Optimization via Optimal Rate Control With Smart Wells. Paper SPE 118948 presented at the SPE Reservoir Simulation Symposium, The Woodlands, Texas, 2-4 February. DOI: 10.2118/118948-MS.

Arenas A. and Dolle N. 2003. Smart Waterflooding Tight Fractured Reservoirs Using Inflow Control Valves. Paper SPE 84193 presented at the SPE annual Technical Conference and Exhibition, Denver, Colorado, 5-8 October. DOI: 10.2118/84193-MS.

Bickel, J. Eric, Richard L. Gibson, Duane A. McVay, Stephen Pickering, and John Waggoner. 2006. Quantifying the Reliability and Value of 3D Land Seismic. SPEREE 11 (5): 832-841. SPE: 102340-PA. DOI: 10.2118/102340-PA.

Brouwer, D.R., Jansen, J.D., Van der Starre, S., van Kruijsdijk, C.P.J.W. and Berentsen, C.W.J. 2001. Recovery Increase Through Waterflooding With Smart Well Technology. Paper SPE 68979 presented at the SPE European Formation Damage Conference, The Hague, The Netherlands, 21-22 May. DOI: 10.2118/68979-MS.

Brouwer, D. R. and Jansen, J.D. 2004. Dynamic Optimization of Waterflooding With Smart Wells Using Optimal Control Theory. *SPE J.* **9** (4):391-402. SPE: 78278-PA. DOI: 10.2118/78278-PA.

Cheng, H., Kharghoria, A., He, Z., and Datta-gupta, A. 2005a. Fast History Matching of Finite-Difference Models Using Streamline-Derived Sensitivities. *SPEREE* **8** (5): 426-436. SPE: 89447-PA. DOI: 10.2118/89447-PA.

Cheng, H. Datta-Gupta, A., and He, Z. 2005b. A Comparison of Travel-Time and Amplitude Matching for Field-Scale Production-Data Integration: Sensitivity, Nonlinearity, and Practical Implications. *SPE J.* **10** (1): 75-90. SPE: 84570-PA. DOI: 10.2118/84570-PA.

Craig, Forrest F. 1971. The Reservoir Engineering Aspects of Waterflooding. Monogragh Series, SPE, Richardson, Texas, Page 13-35.

Datta-Gupta, A. and King, M. J. 2007. Streamline Simulation: Theory and Practice. Textbook Series, SPE, Richardson, Texas, Page 8-24.

ECLIPSE File Formats Reference Manual 2007, Houston, Texas, Schlumberger Information Solutions.

Emerick, A.A., Portella, R.C.M., and Petrobras, S. A. 2007. Production Optimization With Intelligent Wells. Paper SPE 107261 presented at Latin American & Caribbean Petroleum Engineering Conference, Buenos Aires, Argentina, 15-18 April. DOI: 10.2118/107261-MS.

Glandt, C. A. 2003. Reservoir Aspects of Smart Wells. Paper SPE 81107 presented at the SPE Latin American and Caribbean Petroleum Engineering Conference, Port-of-Spain, Trinidad, West Indies, 27-30 April. DOI: 10.2118/81107-MS.

Guyaguler, B., Horne, R. N. 2001. Uncertainty assessment of Well Placement Optimization. Paper SPE 71625 presented at the SPE Annual Technical Conference and Exhibition, New Orleans, Louisiana, 30 September-3 October. DOI: 10.2118/71625-MS.

Hussain, A., Kumar A., Garni, S.A., and Shammari, M.A. 2005. Optimizing Maximum-Reservoir-Contact Wells: Application to Saudi Arabian Reservoirs. Paper IPTC 10395 presented in the International Petroleum Technology Conference, Doha, Qatar, 21-23 November. DOI: 10.2523/10395-MS.

Lake L W., Schmidt R. L., and Venuto P. B. 1992. A Niche for Enhanced Oil Recovery in the 1990s. Oilfield Review: Schlumberger Publication: 55-61, January.

Nocedal, J. and Wright, S. J. 2006: *Numerical Optimization*, 2nd ed. New York: Springer Science + Business Media.

Peters, L., Arts, R.J., Brouwer, G.K., and Gell, C. 2009. Results of the Brugge Benchmark Study for flooding Optimization and History Matching. Paper SPE 119094 presented at the SPE Reservoir Simulation Symposium, The Woodlands, Texas, USA, 2–4 February. DOI: 10.2118/119094-MS.

Sarma, P., Durlofsky, L. J., and Aziz, K. 2005. Efficient Closed-loop Production Optimization under Uncertainty. Paper SPE 94241 presented at the Europec/EAGE annual Conference, Madrid, Spain, 13-16 June. DOI: 10.2118/94241-MS.

Simpson, G. S. Lamb, F. E., Finch, J. H., and Dinnie, N. C. 2000. The Application of Probabilistic and Qualitative Methods to Asset Management Decision Making. Paper SPE 59455 presented in the SPE Asia Pacific Conference on Integrated Modeling for Asset Management, Yokohama, Japan, 25-26 April. DOI: 10.2118/59455-MS.

Sudaryanto, B. and Yortsos, Y.C. 2001. Optimization of Displacements in Porous Media Using Rate Control. Paper SPE 71509 presented at the SPE Annual Technical Conference and Exhibition, New Orleans, Louisiana, 30 September-3 October. DOI: 10.2118/71509-MS.

Tavakkolian, M. Jalali, F., and Amadi, M. A. 2004. Production Optimization Using Genetic Algorithm Approach. Paper SPE 88901 presented at the Annual SPE International Technical Conference Exhibition, Abuja, Nigeria, 2-4 August. DOI: 10.2118/88901-MS.

Yeten, B., Durlofsky, L.J. and Aziz, K. 2003. Optimization of Nonconventional Well Type, Location, and Trajectory. *SPE J.* **8** (3): 200-210. SPE: 86880-PA. DOI: 10.2118/86880-PA.

APPENDIX A

DERIVATION OF ANALYTICAL SENSITIVITY

The arrival time to a producer is defined as the time required for the waterfront to reach the producer from its current position.

$$t_{i,m}^{k} = \left(\frac{1}{N_{fsl,i}} \sum_{l=1}^{N_{fsl,i}} \tau_{l,i} \Big/ \left[\frac{df_w}{dS_w} \right]_{S_w = S_{wf,l}} \right)^{k} \quad \text{.....(A.1)}$$

In the above expression, $N_{fsl,i}$ represents the number of the fastest streamlines connected to the producer i belonging to group m. As mentioned, we choose a set of the fastest streamlines which consists a portion of $N_{sl,i}$, where $N_{sl,i}$ is the total number of streamlines connected to the producer i. The variable τ represents the usual streamline time-of-flight defined as,

$$\tau = \int_{\Sigma} s(\mathbf{x})\, dx \quad \text{.....(A.2)}$$

where the integral is along the streamline trajectory, $\sum$ and $s(\mathrm{x})$ is the 'slowness' defined as the reciprocal of the total interstitial velocity

$$s(\mathbf{x}) = \frac{1}{|v(\mathbf{x})|} = \frac{A(\mathbf{x})\phi(\mathbf{x})}{q_{sl}} \quad \text{.....(A.3)}$$

The variables q_{sl}, $A(\mathbf{x})$ and $\phi(\mathbf{x})$ represent the flow rate, streamtube area, and porosity along individual streamlines. Note that Eq. A.1 acknowledges that the travel time of the waterfront is related to the streamline time of flight through the fractional flow relationship.

The desired arrival time should be the same for all producers within group *m*. The desired arrival time, $t_{d,m}^{k}$ for group *m* at iteration *k* is chosen so as to minimize the variance as follows:

$$\min_{t_{d,m}^{k}} \frac{1}{N_{prod,m}} \sum_{i=1}^{N_{prod,m}} \left(t_{d,m}^{k} - t_{i,m}(\mathbf{q}^{k}) \right)^{2} \quad \text{.....(A.4)}$$

which results in the following,

$$t_{d,m}^{k} = \frac{\sum_{i}^{N_{prod,m}} t_{i,m}(\mathbf{q}^{k})}{N_{prod,m}} \quad \text{.....(A.5)}$$

The next step is to compute the coefficients of the sensitivity matrix S_{ij} analytically. By Combining Eqs. 2.9 and A.1, we can write S_{ij} as follows,

$$S_{ij} = \frac{1}{N_{fsl,i}} \sum_{l=1}^{N_{fsl,i}} \frac{\partial \tau_{l,i}}{\partial q_{j}} \Big/ \left[\frac{df_{w}}{dS_{w}} \right]_{S_{w}=S_{wf,l}} \quad \text{.....(A.6)}$$

Using the chain rule, the partial derivative in Eq. A.6 can be written as

$$\frac{\partial \tau_{l,i}}{\partial q_{j}} = \frac{\partial \tau_{l,i}}{\partial q_{sl,i}} \frac{\partial q_{sl,i}}{\partial q_{j}} \quad \text{.....(A.7)}$$

The expression $\partial \tau_{l,i} / \partial q_{sl,i}$ represents the change in time of flight along individual streamlines connected to producer *i* because of changes in the total flow rate along the streamline. If we assume that the streamlines do not shift because of small perturbations in wells rate, then this partial derivative can be computed analytically using Eq. A.2 and Eq. A.3.

$$\frac{\partial \tau_{l,i}}{\partial q_{sl,i}} = \int_{\Sigma} \frac{\partial s(\mathbf{x})}{\partial q_{sl,i}}\, dx = -\int_{\Sigma} \frac{s(\mathbf{x})}{q_{sl,i}}\, dx = -\frac{\tau_{l,i}}{q_{sl,i}} \quad \text{.....(A.8)}$$

The second partial derivative in Eq. A.7, ($\partial q_{sl,i} / \partial q_j$) represent the change in the total production rate along a streamline connected to producer *i* because of a change in the total rate of well *j*. Recall that well *j* can be either a producer or an injector. Let's consider first the case when it is a producer. In this case, the derivative will vanish for $i \neq j$ because of the assumption that the streamlines do not shift for small perturbations in well rates. If *i=j*, the well rate and the flow rate along individual streamline are related as follows,

$$q_i = N_{sl,i} q_{sl,i} \quad \text{.....(A.9)}$$

Using Eqs. A.8 and A.9, we can now rewrite Eq. A.7 as

$$\begin{aligned} &\frac{\partial \tau_{sl,i}}{\partial q_j} = -\frac{\tau_{sl,i}}{q_j} \quad \forall i = j \\ &\frac{\partial \tau_{s,i}}{\partial q_j} = 0 \quad \forall i \neq j \end{aligned} \quad \text{.....(A.10)}$$

After substituting Eq. A.10 in Eq. A.6, we have the analytical form of the sensitivities with respect to production rates.

$$\begin{aligned} &S_{ij} = -\frac{t_{i,m}}{q_j} \quad \forall i = j \\ &S_{ij} = 0 \quad \forall i \neq j \end{aligned} \quad \text{.....(A.11)}$$

where j is a producer.

In Eq. A.11, we assume that $t_{i,m}$ is sensitive only to the production of producer *i*. The sensitivity of $t_{i,m}$ is negligible with respect to other producers.

Similar assumptions hold when computing the sensitivity with respect to injection rates. Following a similar approach, the analytical sensitivity with respect to the injection rate can be written as follows,

$$S_{ij} = -\frac{\sum_{l=1}^{N_{fsl,i,j}} \tau_{l,i,j} \Big/ \left[\frac{df_w}{dS_w}\right]_{S_w=S_{wf,l}}}{q_j N_{fsl,i}} \quad if \quad N_{fsl,i,j} \neq 0 \quad \text{.....(A.12)}$$

$$S_{ij} = 0 \quad if \quad N_{fsl,i,j} = 0$$

where j is an injector.

APPENDIX B

DERIVATION OF OBJECTIVE FUNCTION FOR MULTIPLE REALIZATIONS

In this section, we discuss the underlying mathematical formulation for computing optimal injection and production rates given multiple geologic models. First, we present the formulation of the objective function, and then discuss the minimization algorithm and the derivation of the analytical gradient and the Hessian of the objective function.

B.1 Objective Function Formulation

Our main objective is to maximize the sweep efficiency in waterflooding project through rate allocation. We accomplish this by equalizing the arrival time of the waterfront at the producers. Mathematically, this requires minimizing an appropriately defined misfit function for a specific group of producers. For a single realization j, we can formulate the misfit function as the square of the l_2 norm of the residuals,

$$\mathbf{e}_j^T \mathbf{e}_j = \sum_{m=1}^{N_{group}} \sum_{i=1}^{N_{prod,m}} \left(t_{d,m}(\mathbf{q}) - t_{i,m}(\mathbf{q}) \right)^2 \quad \text{.....(B.1)}$$

The arrival time residuals are represented by the vector **e** in Eq. B.1. The variable $t_{i,m}$ represents the calculated arrival time at well *i*, belonging to group *m.* The desired arrival time, $t_{d,m}$ for the well group *m* is given by the arithmetic average of $t_{i,m}$ for each

iteration during the optimization. The vector **q** contains the control variables and has a dimension of *n*, the number of well rates to be optimized.

To address geologic uncertainty, Eq. B.1 needs to be generalized to handle multiple realizations. In this paper, we will use two forms of the objective function to address uncertainty. The first one is a stochastic formulation in terms of an expected value of the misfit in Eq. B.1 for multiple realizations penalized by its standard deviation as follows,

$$f(\mathbf{q}) = \mathrm{E}\left[\mathbf{e}^T\mathbf{e}\right] + r\,\sigma\left[\mathbf{e}^T\mathbf{e}\right] \quad \text{.....(B.2)}$$

Eq. 3.2 can be derived within the decision analysis framework (Bickel et. al. 2006; Guyaguler and Horne 2001; Simpson et. al. 2000; Yeten et. al. 2003). The variable *r* is the risk coefficient that weights the trade off between the expected value and the standard deviation. A positive *r* means that the decision maker is risk averse, while a negative *r* means that the decision maker is risk prone. A zero risk coefficient indicates that the decision maker is risk neutral. The expected value and the standard deviation are given by the following equations,

$$\begin{aligned} \mathrm{E}\left[\mathbf{e}^T\mathbf{e}\right] &= \frac{1}{N_r}\sum_{i=1}^{Nr}\mathbf{e}_i^T\mathbf{e}_i \\ \sigma\left[\mathbf{e}^T\mathbf{e}\right] &= \sqrt{Var(\mathbf{e}^T\mathbf{e})} = \left[\mathrm{E}\left[\left(\mathbf{e}^T\mathbf{e}\right)^2\right] - \mathrm{E}^2\left[\mathbf{e}^T\mathbf{e}\right]\right]^{1/2} \end{aligned} \quad \text{.....(B.3)}$$

The variable N_r in Eq. B.3 refers to the number of realizations used in the optimization. Our goal is to minimize Eq. B.2 by changing **q**, the injection/production

rates, subject to multiple equality and inequality constraints imposed by the operational restrictions and facility limitations. Thus,

$$\min_{\mathbf{q}} f(\mathbf{q}) \quad \text{.....(B.4)}$$

subject to

$$\mathbf{h}(\mathbf{q}) = 0$$
$$\mathbf{g}(\mathbf{q}) \leq 0$$

where $h : \Re^n \rightarrow \Re^z$ and $g : \Re^n \rightarrow \Re^y$

The superscripts z and y represent the number of equality and inequality constraints respectively.

For our application, we assume that the constraints are linear and they have the following forms:

$$\mathbf{h(q) = Aq + b}$$
$$\mathbf{g(q) = Cq + d} \quad \text{.....(B.5)}$$

B.2 Objective Function Minimization

In this section, we discuss the approaches to minimize Eq. B.4. It can be minimized using the sequential quadratic programming (SQP) algorithm for non-linear constrained optimization (Nocedal and Wright 2006). The main concept behind the approach is to formulate the problem into a series of quadratic programming (QP) sub-problems which

can be solved at each major iteration *k*. The QP sub-problem is mainly a quadratic approximation of the Lagrangian of Eq. B.4 which is given in the following form:

$$L(\mathbf{q},\boldsymbol{\lambda}_L,\boldsymbol{\lambda}_K) = f(\mathbf{q}) + \boldsymbol{\lambda}_L^T \mathbf{h}(\mathbf{q}) + \boldsymbol{\lambda}_K^T \mathbf{g}(\mathbf{q}) \quad \text{.....(B.6)}$$

The vectors $\boldsymbol{\lambda}_L$ and $\boldsymbol{\lambda}_K$ refer to the Lagrange multipliers corresponding to the equality constraints and the Karush-Kuhn-Tucker multipliers corresponding to the inequality constraints. After linearizing the constraints using a Taylor approximation, the QP sub-problem can be written as:

$$\min_{\delta\mathbf{q}} \; f(\mathbf{q}^k) + \nabla_q f^T(\mathbf{q}^k)\delta\mathbf{q} + \frac{1}{2}\delta\mathbf{q}\nabla_q^2 L(\mathbf{q}^k)\delta\mathbf{q} \quad \text{.....(B.7)}$$

subject to

$$\mathbf{h}(\mathbf{q}^k) + \nabla_q \mathbf{h}(\mathbf{q}^k)^T \delta\mathbf{q} = 0$$
$$\mathbf{g}(\mathbf{q}^k) + \nabla_q \mathbf{g}(\mathbf{q}^k)^T \delta\mathbf{q} \le 0$$

Eq. B.7 indicates that we need to evaluate the following terms at each iteration to minimize Eq. B.4:

- The objective function : $f(\mathbf{q}^k)$
- The gradient of the objective function : $\nabla_q f(\mathbf{q}^k)$
- The Hessian of the Lagrangian: $\nabla_q^2 L(\mathbf{q}^k)$. This term is equal to the Hessian of the objective function, $\nabla_q^2 f(\mathbf{q}^k)$, given that the constraints are linear.

- The gradient of the constraints: $\nabla_q \mathbf{h}\left(\mathbf{q}^k\right)$ and $\nabla_q \mathbf{g}(\mathbf{q}^k)$

The objective function evaluation relies mainly on the computation of the residuals for each realization. A complete discussion on the derivation of waterfront arrival time and the desired arrival time can be referred in Appendix A. The gradient of the constraints are straightforward because we assumed that they are linear with respect to the control variable. The computation of the gradient and Hessian of the objective function will be discussed in the next section.

B.3 Objective Function Gradients and Hessian

The gradient of the objective function in Eq. B.2 is given by the following expression:

$$\nabla_q f(\mathbf{q}) = 2\mathrm{E}\left[\mathbf{J}^T\mathbf{e}\right] + 2\, r\, \frac{\mathbf{Cov}\left(\mathbf{e}^T\mathbf{e},\mathbf{J}^T\mathbf{e}\right)}{\sigma\left(\mathbf{e}^T\mathbf{e}\right)} \quad \text{.....(B.8)}$$

The first term in Eq. B.8, E[$\mathbf{J}^T\mathbf{e}$], represents the expected value of the gradient of the misfit function in Eq. B.1 computed for each realization. The second term contains **Cov**($\mathbf{e}^T\mathbf{e}$, $\mathbf{J}^T\mathbf{e}$) which represents the cross-covariance vector of the misfit and its gradient computed for each realization. For illustration, a single element with an index *i* in the cross covariance vector is given by the following expression:

$$Cov_i = Cov\left(\mathbf{e}^T\mathbf{e},(\mathbf{J}^T\mathbf{e})_i\right) \quad \text{.....(B.9)}$$

The expression in Eq. B.9 indicates that an element *i* can be obtained by computing the cross covariance between two vectors. The first term is the misfit function

in Eq. B.1 for each realization and the second term is the i^{th} element of the gradient evaluated for each realization.

The Hessian of the objective function in Eq. B.2 is given by,

$$\nabla_q^2 f(\mathbf{q}) = 2\mathrm{E}\left[\mathbf{J}^T\mathbf{J}\right] + r\frac{4\,\mathbf{Cov}\left(\mathbf{J}^T\mathbf{e},\mathbf{J}^T\mathbf{e}\right)+2\mathbf{Cov}\left(\mathbf{e}^T\mathbf{e},\mathbf{J}^T\mathbf{J}\right)}{\sigma(\mathbf{e}^T\mathbf{e})} - r\frac{4\;\mathbf{Cov}\left(\mathbf{e}^T\mathbf{e},\mathbf{J}^T\mathbf{e}\right)\;\mathbf{Cov}^T\left(\mathbf{e}^T\mathbf{e},\mathbf{J}^T\mathbf{e}\right)}{\sigma^3(\mathbf{e}^T\mathbf{e})} \quad \text{.....(B.10)}$$

The first term, $\mathrm{E}[\mathbf{J}^T\mathbf{J}]$ is the expected value of Hessian of the square of the l_2 norm of the residuals computed for each realization. $\mathbf{Cov}(\mathbf{J}^T\mathbf{e}, \mathbf{J}^T\mathbf{e})$ is the covariance matrix for the gradients vectors obtained from each realization. A single element in this matrix can be obtained using the following expression:

$$Cov_{ij} = Cov\left((\mathbf{J}^T\mathbf{e})_i,(\mathbf{J}^T\mathbf{e})_j\right) \quad \text{.....(B.11)}$$

This expression means that an *ij*-element where *i* is the row index and *j* is the column index, is evaluated by computing the covariance between two series of numbers. The first one represents the i^{th} element of each gradient vector, and the second series represents the j^{th} element of each gradient vector. $\mathbf{Cov}(\mathbf{e}^T\mathbf{e}, \mathbf{J}^T\mathbf{J})$ is a cross covariance matrix between the square of the l_2 norm of the residuals evaluated for each realization and the Hessian of the l_2 norm of the residuals computed for each realization. An element in this matrix, Cov_{ij}, is computed using the following expression:

$$Cov_{ij} = Cov\left(\mathbf{e}^T\mathbf{e},(\mathbf{J}^T\mathbf{J})_{ij}\right) \quad \text{.....(B.12)}$$

The above expression indicates that a single element located at *ij*-index is computed by a cross-covariance between two series of numbers. The first series is the square of the l_2 norm for each realization, and the second one is the *ij*-elements of the Hessian matrix computed for each realization.

B.4 Jacobian Matrix and Analytical Sensitivity Calculations

In this section, we show the computation of the Jacobian matrix, J, for each realization. The Jacobian is given by the following expression:

$$\mathbf{J}=\nabla_q \mathbf{e} \quad \text{(B.13)}$$

A single element in the residual vector, **e**, can be written as follows:

$$e_{i,m}=t_{d,m}(\mathbf{q})-t_{i,m}(\mathbf{q}) \quad \text{(B.14)}$$

Eq. B.14 refers to the arrival time residual at producer *i*. By combining Eq. A.5, B.13, and B.14, a single element in the Jacobian matrix can be written as,

$$J_{ij}=\left[\frac{1}{N_{Group}}\sum_{k=1}^{N_{Group}} S_{kj}\right]-S_{ij} \quad \text{(B.15)}$$

The sensitivity coefficient S_{ij} quantifies the changes in arrival time at producer *i* because of small changes in the rate of well *j*. It is given by

$$S_{ij} = \frac{\partial t_{i,m}(\mathbf{q})}{\partial q_j} \quad \text{.....(B.16)}$$

If the derivative is taken with respect to the rate of a producer, the sensitivity coefficient is given by the following expression:

$$\begin{aligned} S_{ij} &= -\frac{t_{i,m}}{q_j} \quad \forall i = j \\ S_{ij} &= 0 \quad \forall i \neq j \end{aligned} \quad \text{.....(B.17)}$$

where j is a producer.

In Eq. B.17, we assume that $t_{i,m}$ is sensitive only to the production of producer i. The sensitivity of $t_{i,m}$ is considered to be negligible with respect to the rates of other producers.

If the derivative is taken with respect to the rate of an injector, the sensitivity coefficient can be written as follows:

$$\begin{aligned} S_{ij} &= -\frac{\sum_{l=1}^{N_{fsl,i,j}} \tau_{l,i,j} \Big/ \left[\frac{df_w}{dS_w}\right]_{S_w = S_{wf,l}}}{q_j N_{fsl,i}} \quad if \quad N_{fsl,i,j} \neq 0 \\ S_{ij} &= 0 \quad if \quad N_{fsl,i,j} = 0 \end{aligned} \quad \text{.....(B.18)}$$

where j is an injector.

The variable $N_{fsl,i,j}$ is the number of the fast streamlines connecting a producer i to an injector j. This number represents only a fraction of $N_{fsl,i}$ the total number of the

fastest streamlines connected to the producer *i*. If the injector *j* is not connected to producer *i* through a fast streamline i.e. ($N_{fsl,i,j}$=0), then the arrival time at producer *i* is not sensitive to a perturbation in the rate of injector *j*.

VITA

Qing Tao received his Bachelor of Science degree in engineering physics from Tsinghua University, China in 2007. He entered the petroleum engineering graduate program at Texas A&M University and received his Master of Science degree in December 2009. His research interests include reservoir simulation and production optimization. His mailing address is: Harold Vance Department of Petroleum Engineering, Texas A&M University, College Station, TX 77843-3116. His email is: taoqing222@gmail.com.